

The Empirical Implications of the Interest-Rate Lower Bound

Christopher Gust

David López-Salido

Matthew E. Smith*

First Draft: November 2012

This Draft: February 2013

Abstract

Using Bayesian methods, we estimate a nonlinear DSGE model in which the interest-rate lower bound is occasionally binding. We quantify the size and nature of disturbances that pushed the U.S. economy to the lower bound in late 2008 as well as the contribution of the lower bound constraint to the resulting economic slump. Compared with the hypothetical situation in which monetary policy can act in an unconstrained fashion, our estimates imply that U.S. output was more than 1 percent lower, on average, over the 2009–2011 period. Moreover, around 20 percent of the drop in U.S. GDP during the recession of 2008–2009 was due to the interest-rate lower bound. We show that the estimated model generates lower bound episodes that resemble salient characteristics of the observed U.S. episode, including its expected duration.

Keywords: zero lower bound, DSGE model, Bayesian estimation

JEL classification: C11, C32, E32, E52

*Federal Reserve Board. Email Addresses: christopher.gust@frb.gov; david.lopez-salido@frb.gov; and matthew.smith@frb.gov, respectively. We thank Larry Christiano, Luca Guerrieri, Wouter den Haan, Matteo Iacoviello, Mike Kiley, André Kurmann, Karel Mertens, Tai Nakata, Ed Nelson, Chris Sims, Rob Vigfusson, and Tao Zha for helpful comments, and Christine Garnier for excellent research assistance. The views expressed in this paper are solely the responsibility of the authors and should not be interpreted as reflecting the views of the Board of Governors of the Federal Reserve System or of any other person associated with the Federal Reserve System.

1 Introduction

The last five years have witnessed a return of near-zero interest rates in many advanced economies. As a result of the recent financial crisis, the United States and other advanced economies joined Japan, experiencing a protracted period in which the lower bound constraint on nominal interest rates became a practical concern for policymakers. At the same time, researchers have been actively developing and applying dynamic stochastic general equilibrium (DSGE) models in order to understand how the economy works and responds to alternative policies under these circumstances.¹ Because of the nonlinearity inherently entailed by the lower bound, a more challenging task has been to estimate a model incorporating this constraint. Accordingly, the empirical evidence regarding the role of the lower bound constraint has been limited.

To investigate the importance of this constraint on the macroeconomy, this paper estimates a nonlinear DSGE model in which the interest-rate lower bound is occasionally binding. Although we apply this methodology to the interest-rate lower bound, our approach is more general and could be used in many different contexts, including models with financial constraints. When applied to the interest-rate lower bound, the technique allows us to identify the nature and size of disturbances that pushed the interest rate to the lower bound in the United States in late 2008 and quantify the role of the constraint in exacerbating the resulting economic slump. We also quantify the likelihood of a zero lower bound event and its duration as well as the role that systematic monetary policy plays in affecting its likelihood and duration.

We estimate a nonlinear version of a model widely used in monetary economics and macroeconomics. The model is tractable but rich enough to provide an interpretation of recent economic developments of the U.S. economy. The model's key features include habit persistence in preferences, which helps deliver empirically-realistic dynamics, and price adjustment costs that make firms unwilling to make a complete immediate adjustment of nominal prices. In addition, monetary policy is governed by an interest rate rule that responds to changes in inflation, output growth, and the lagged interest rate; however, that policy is constrained by the lower bound.

Economic fluctuations in the model are driven by three aggregate disturbances: productivity shocks, monetary policy innovations, and—following Eggertsson and Woodford (2003) and Christiano, Eichen-

¹ See, for instance, Eggertsson and Woodford (2003), Christiano, Eichenbaum, and Rebelo (2011), Basu and Bundick (2012), and Fernandez-Villaverde, Gordon, Guerron-Quintana, and Rubio-Ramirez (2012).

baum, and Rebelo (2011)—a shock to the economy’s discount rate. The latter shock can increase an agents propensity to save, reducing current spending and the aggregate price level. We view this shock as standing in for a wide variety of factors that alter households’ propensity to save that we do not explicitly model—including, for example, both financial and uncertainty shocks.

In the model, the lower bound constraint is potentially an important factor influencing the stance of monetary policy and hence economic behavior. By constraining the current interest rate, the lower bound may limit the degree of monetary stimulus. However, monetary policy can still be effective in influencing expectations about future output and inflation, thereby affecting the current level of prices and spending. Similarly, the current decisions of households and firms are influenced by the expectation that in future states the constraint may be binding.

Our solution algorithm takes into account the effect that uncertainty about the likelihood that the economy will be at the lower bound has on economic decisions of households and firms. In particular, following Christiano and Fisher (2000), the stochastic, nonlinear model is solved using a projection method, after which we estimate the nonlinear model using Bayesian methods.² With these techniques, draws from the posterior distribution of parameters given the data are typically produced by constructing a Markov chain using the Metropolis-Hastings algorithm. Our nonlinear solution method yields a nonlinear state space system that requires a particle filter to evaluate the likelihood function.³ In the standard implementation of the Metropolis-Hastings algorithm, at each iteration the economic model must be solved and the likelihood function must be evaluated at the vector of proposed parameter values. In the context of our model, these two computationally intensive tasks leave a standard Random-Walk implementation of the Metropolis-Hastings algorithm impractical.

Instead of the standard Random-Walk implementation, we follow Smith (2011), who introduces a surrogate into the Metropolis-Hastings algorithm. The idea underlying the procedure in Smith (2011) is that different ways of solving an economic model yield different likelihood functions, and one can exploit easy-to-compute likelihood functions to ‘pre-screen’ proposed parameter configurations using some first stage acceptance criteria. This easy-to-compute likelihood function is called a *surrogate*. Only after the parameters have been accepted in the first step is the nonlinear model solved and the likelihood function evaluated using the particle filter. The algorithm produces draws from the posterior

² The use of Bayesian techniques to estimate linearized versions of DSGE models has increased in recent years. See An and Schorfheide (2007) for a recent survey of the literature.

³ See Fernandez-Villaverde and Rubio-Ramirez (2007) for the first application of a particle filter to estimate a nonlinear DSGE model.

distribution of parameters computed from the nonlinear solution method, but is substantially faster than a standard Random-Walk algorithm. In the present context, the surrogate is constructed by linearizing the equilibrium conditions of the model and using a Kalman filter to evaluate the surrogate likelihood function.

We use this technique to estimate the nonlinear model using U.S. quarterly data on output growth, inflation, and the nominal interest rate from 1983 through 2011. For this sample period, there is a single episode spanning from 2009 until the end of the sample, in which the nominal interest rate is effectively at the lower bound. We examine the model’s estimated shocks during this episode and use them to construct empirically relevant initial conditions. This approach allows us to demonstrate how such conditions determine the likelihood and severity of a lower bound event as well as alter the propagation of the economy’s shocks.

For the episode in which the interest rate was at the lower bound, a substantial fall in private demand or in the discount rate during the ‘Great Recession’, 2008–2009, was the key force pushing the interest rate to the lower bound. The productivity shock also contributed to the large initial outcome contraction at the end of 2008 and remained low, on average, through 2010.⁴ However, the large and persistent fall in the discount rate shock was relatively more important in explaining the response of inflation and the nominal interest rate during the episode, while also contributing to the slow growth during this period. In addition, we find that the monetary shocks contributed little to the dynamics of inflation, output, and the nominal interest rate in the course of this episode and were generally small over our entire sample.

Using these estimates of the shocks, a central question we address is how much did the lower bound constrain the ability of monetary policy to stabilize the economy. We answer this question by comparing our estimated model in which the lower bound is imposed to the hypothetical case in which monetary policy can act in an unconstrained manner. In the latter case, the policy rule would have called for a negative nominal interest rate that falls to -4 percent in 2009 and subsequently rises but is still below -1 percent at the end of the sample. This counterfactual experiment implies that U.S. output is about 1 percent lower, on average, from 2009–2011 under the constrained policy rule relative to the hypothetical scenario without the lower bound. In addition, around 20 percent of the drop in U.S. GDP during the Great Recession was due to the interest-rate lower bound.

⁴ Our results on productivity are broadly in line with Fernald (2012), who uses a growth-accounting framework and finds that total factor productivity declined during the Great Recession.

We examine the estimated model’s implications for the probability of hitting the lower bound and the duration of a lower bound spell. While the duration of the U.S. spell at the end of our sample is 12 quarters, expectations of the duration at the beginning of this spell based on financial market data and private sector forecasts were much shorter. Most financial market participants and private sector forecasters anticipated a lower-bound spell of only 3 or 4 quarters in the first quarter of 2009 when the spell had just began. We find that our model is largely in line with these private sector expectations, as the median model forecast in the first quarter of 2009 is that the lower-bound spell lasts for four quarters. Thus, both from the perspective of the model and private sector forecasts, the protracted length of the U.S. lower bound spell was largely unanticipated. Though a spell of 12 quarters or longer occurs relatively infrequently in the model, we show that these long-lasting spells in the model generate outcomes for interest rates, inflation, and output resembling the movements of their empirical counterparts.

Our paper is closely related to other work that has estimated models to quantify the effects of the interest-rate lower bound. One approach has been to estimate a linearized DSGE model without the constraint and then interpret the residuals from the monetary policy rule as reflecting the effect of the constraint (e.g., Ireland (2011)). Such evidence is at best indirect, because these innovations reflect other factors. More importantly, this approach omits how the lower bound systematically changes monetary policy and thus the behavior of economic agents—a key aspect at the heart of our analysis.

Another approach is to estimate a linear model over a sample period in which the constraint does not bind and uses those estimates to simulate a nonlinear version of the model that imposes the constraint.⁵ Our estimation routine extracts information contained in the posterior of the linearized model without assuming that it is identical to the posterior distribution of the fully nonlinear model. In fact, our results suggest that there are important differences between these two posteriors. Moreover, linearizing the model and estimating it on a non binding subsample precludes estimating the shocks that occurred over the lower bound episode and using them to quantify the economic effects of the constraint, a central feature of our analysis.

In a recent paper, Aruoba and Schorfheide (2012) examine the disturbances that took the economy to the lower bound in a New Keynesian model and find that a sunspot shock is important to account for economic behavior at the lower bound. Our model differs from theirs along a number of dimensions

⁵ See, for example, Coenen, Orphanides, and Wieland (2004) and Chung, Laforte, Reifschneider, and Williams (2012), who estimate the probability of a zero lower bound event using this approach.

including the types of shocks, preferences, and the monetary policy rule. Without a sunspot shock, our model can account for most of the observed fall in output and inflation while also generating an expected duration for the lower bound spell consistent with both financial market and survey data. In addition, the authors focus on evaluating alternative policy interventions at the lower bound instead of using the model to quantify the lower bound’s role in exacerbating the Great Recession, a central question that we address.

The rest of the paper proceeds as follows. The next section presents the macroeconomic model that we estimate, while section 3 discusses how the model is solved and estimated. The next three sections present the model’s results. Section 4 discusses the model’s parameter estimates and impulse responses as well as assesses the model’s fit. Section 5 examines the observed lower bound episode in detail, describing the estimated shocks that took the economy to the lower bound and quantifying the contribution of the lower bound to the Great Recession. The results regarding the model’s implications for the probability and duration of lower bound events are presented in Section 6. Section 7 presents some conclusions. The technical details associated with both the solution and the estimation of the model are presented in an appendix.

2 The Model

The economy consists of a continuum of households, a continuum of firms producing differentiated intermediate goods, a perfectly competitive final goods firm, and a central bank in charge of monetary policy. We now lay out the objectives and constraints of the different agents.

2.1 Households

There is a representative household choosing consumption C_t , a one period nominal bond, B_t , and labor services, H_t , that are supplied to the firm. The household seeks to maximize:

$$\max E_t \sum_{t=1}^{\infty} \delta_{t-1} (\log [C_t - \gamma C_{t-1}^a] - H_t) \quad (1)$$

subject to the sequence of budget constraints,

$$P_t C_t + R_t^{-1} B_t = W_t H_t + B_{t-1} + P_t D_t + P_t T_t. \quad (2)$$

Household nominal expenditures on consumption at date t are given by $P_t C_t$, where P_t denotes the aggregate price level. A household also purchases B_t units of the nominal bonds at the price R_t^{-1} , where R_t denotes the gross nominal return on these bonds. The nominal bonds purchased by a household pay one unit of the numéraire next period with certainty. A household receives income from any bonds carried over from last period in addition to its labor income, $W_t H_t$, from supplying its services to the economy's firms. A household also receives dividends, D_t , as an owner of the economy's firms and collects any lump-sum transfers, T_t .

A feature of household preferences as specified in equation (1) are that they are intertemporally non-separable. C_{t-1}^a represents previous period aggregate consumption that the household takes as given, and the parameter $0 \leq \gamma < 1$ captures the importance of these external habits. Habit persistence, as discussed in Christiano, Eichenbaum, and Evans (2005) and Smets and Wouters (2007), allows for hump-shaped output dynamics in response to shocks, improving the model's empirical fit. The linear specification for labor services in equation (1) along with a competitive labor market implies that there is a perfectly elastic supply of labor available to the economy's firms.

We follow Eggertsson and Woodford (2003) and Christiano, Eichenbaum, and Rebelo (2011) in allowing for a shock to the discount rate. The discount factor at time t is given by $\delta_t = \beta^t \left(\prod_{s=0}^t \eta_s \right)^{-1}$, where $0 < \beta < 1$. Hence, $\frac{\delta_{t+1}}{\delta_t} = \frac{\beta}{\eta_{t+1}}$, and η_{t+1} is a shock to the discount rate or the natural rate of interest that alters the weight of the future utility at time $t+1$ in relation to the period utility at time t . The discount rate shock follows an AR(1) process:

$$\log(\eta_t) = \rho_\eta \log(\eta_{t-1}) + \varepsilon_{\eta,t} \quad (3)$$

where ρ_η denotes the persistence of the shock and σ_η denotes the standard deviation of the shock innovations, $\varepsilon_{\eta,t}$. A decrease in η_t represents an exogenous factor that induces a temporary rise in a household's propensity to save, and reduces current aggregate household demand for goods.⁶

The first order conditions for bonds, consumption and labor can be written as follows:

$$\Lambda_t = \frac{\beta}{\eta_t} R_t E_t \Lambda_{t+1} \Pi_{t+1}^{-1}, \quad (4)$$

⁶ In a recent paper, Hall (2011) develop a structural model in which financial shocks act in this manner. In their model, a tightening in household borrowing constraints can induce some consumers to increase their precautionary savings and lead to lower interest rates.

$$w_t = C_t - \gamma C_{t-1}^a \quad (5)$$

where $\Lambda_t = [C_t - \gamma C_{t-1}^a]^{-1}$ is the marginal utility of consumption, $w_t = \frac{W_t}{P_t}$ denotes the real wage, and $\Pi_{t+1} = \frac{P_{t+1}}{P_t}$ is the inflation rate between t and $t+1$. Lastly, in equilibrium, individual and aggregate consumption coincide, $C_t = C_t^a$.

2.2 Firms

There are a continuum of monopolistically competitive firms producing differentiated intermediate goods. The latter are used as inputs by a (perfectly competitive) firm producing a single final good. The final good is produced by a representative, perfectly competitive firm with a constant returns technology, $Y_t = \left(\int_0^1 Y_t(j)^{\frac{\varepsilon-1}{\varepsilon}} dj \right)^{\frac{\varepsilon}{\varepsilon-1}}$, where $Y_t(j)$ is the quantity of intermediate good j used as an input, and $\varepsilon > 1$ is the constant elasticity of substitution. Profit maximization, taking as given the final goods price P_t and the prices for the intermediate goods $P_t(j)$, for all $j \in [0, 1]$, yields the set of demand schedules, $Y_t(j) = \left(\frac{P_t(j)}{P_t} \right)^{-\varepsilon} Y_t$. Finally, the zero profit condition yields the price index: $P_t = \left(\int_0^1 P_t(j)^{1-\varepsilon} dj \right)^{\frac{1}{1-\varepsilon}}$.

The production function for intermediate good j is given by:

$$Y_t(j) = Z_t H_t(j), \quad (6)$$

where Z_t represents total factor productivity, and $H_t(j)$ represents the labor services hired by firm j . We assume that Z_t follows a random walk with drift:

$$\ln(Z_t) = \log(G) + \ln(Z_{t-1}) + \varepsilon_{Z,t}, \quad (7)$$

where G is the unconditional (gross) rate of growth in productivity. The variable $\varepsilon_{Z,t}$ is a random productivity shock with zero mean and standard deviation, σ_Z .

Since intermediate goods substitute imperfectly for one another, the representative intermediate goods-producing firm sells its output in a monopolistically competitive market. During period t , the firm sets its nominal price $P_t(j)$, subject to the requirement that it satisfies the demand of the representative final goods producer at that price. Following Rotemberg (1982), the intermediate good producer faces a quadratic cost of adjusting its nominal price between periods, measured in terms of

the finished good and given by: $\frac{\varphi}{2} \left[\frac{P_t(j)}{\bar{\Pi}P_{t-1}(j)} - 1 \right]^2 Y_t$, where φ governs the obstacles to price adjustment and $\bar{\Pi}$ is the central bank's inflation target. The cost of price adjustment makes the problem of the intermediate good producer dynamic; that is, it chooses $P_t(j)$ to maximize its present discounted value of expected profits:

$$E_0 \sum_{t=1}^{\infty} \delta_{t-1} \Lambda_t \left[\left(\frac{P_t(j)}{P_t} \right)^{1-\varepsilon} Y_t - \left(\frac{P_t(j)}{P_t} \right)^{-\varepsilon} w_t Y_t - \frac{\varphi}{2} \left[\frac{P_t(j)}{\bar{\Pi}P_{t-1}(j)} - 1 \right]^2 Y_t \right],$$

where $\delta_{t-1} \Lambda_t$ measures the marginal value—in utility terms—to the representative household of an additional unit of real profits received in the form of dividends during period t and w_t is the firm's real marginal cost given that the production function is linear in labor. The first order conditions for this problem are:

$$(1 - \varepsilon) \left(\frac{P_t(j)}{P_t} \right)^{-\varepsilon} + \varepsilon \left(\frac{P_t(j)}{P_t} \right)^{-\varepsilon-1} w_t - \varphi \left[\frac{P_t(j)}{\bar{\Pi}P_{t-1}(j)} - 1 \right] \frac{P_t(j)}{\bar{\Pi}P_{t-1}(j)} + \varphi \frac{\beta}{\eta_t} E_t \left\{ \frac{\Lambda_{t+1}}{\Lambda_t} \left[\frac{P_{t+1}(j)}{\bar{\Pi}P_t(j)} - 1 \right] \frac{P_{t+1}(j)}{\bar{\Pi}P_t(j)} \frac{P_t}{P_t(j)} \frac{Y_{t+1}}{Y_t} \right\} = 0. \quad (8)$$

2.3 Monetary Policy

The central bank is assumed to set the nominal interest rate R_t each period according to an interest rate rule:

$$R_t = \max[\bar{R}, R_t^*] \quad (9)$$

where,

$$R_t^* = \left(\frac{\bar{\Pi}G}{\beta} \right)^{1-\rho_R} (R_{t-1}^*)^{\rho_R} \left(\frac{\Pi_t}{\bar{\Pi}} \right)^{\gamma_\pi} \left(\frac{Y_t}{GY_{t-1}} \right)^{\gamma_y} \exp(\varepsilon_{R,t}). \quad (10)$$

In the above, \bar{R} denotes the effective lower bound on R_t , which in practice the central bank may set above 1, while R_t^* denotes a central bank's desired or notional interest rate that it would choose to set in the absence of the lower bound constraint.⁷ The desired policy rate responds to its lag, the inflation rate less the central bank's target, $\bar{\Pi}$, and output growth with coefficients ρ_R , γ_π , and γ_y , respectively. The variable $\varepsilon_{R,t}$ is a white noise monetary policy shock with zero mean and standard deviation, σ_R . Finally, it is assumed that any seigniorage income earned by the central bank is rebated back to the

⁷ Since December 2008 the Federal Open Market Committee's (FOMC) target federal funds rate has actually been slightly above zero, reflecting concerns about the functioning of money market funds. However, we set $\bar{R} = 1$ for the estimation routine.

households in a lump-sum fashion.

2.4 Market Clearing and Aggregate Equilibrium

In symmetric equilibrium, all intermediate goods producing firms make the same decisions so that aggregate output satisfies $Y_t = Y_t(j)$ and aggregate labor satisfies $H_t = H_t(j) \forall j$. It then follows that $Y_t = Z_t H_t$ and goods market clearing can be written in aggregate terms as:

$$Y_t = C_t + \frac{\varphi}{2} \left(\frac{\Pi_t}{\bar{\Pi}} - 1 \right)^2 Y_t. \quad (11)$$

Households trade the nominal bond amongst themselves so that bond market clearing implies $B_t = 0$.

The random walk in the technology shock, expression (7), implies that some of the variables will inherit a unit root. As a result, it is convenient to define stationary representations of output, consumption, and the marginal utility of consumption as follows: $\tilde{Y}_t = \frac{Y_t}{Z_t}$, $\tilde{C}_t = \frac{C_t}{Z_t}$, and $\tilde{\lambda}_t = Z_t \Lambda_t$. Rewriting the equilibrium conditions from households and firms as well as the goods market clearing condition in terms of the scaled variables yields:

$$\tilde{\lambda}_t = \frac{\beta R_t}{G \eta_t} E_t \left\{ \tilde{\lambda}_{t+1} \Pi_{t+1}^{-1} \exp(-\varepsilon_{Z,t+1}) \right\} \quad (12)$$

$$\tilde{Y}_t = \tilde{C}_t + \frac{\varphi}{2} \left(\frac{\Pi_t}{\bar{\Pi}} - 1 \right)^2 \tilde{Y}_t \quad (13)$$

$$\varphi \left(\frac{\Pi_t}{\bar{\Pi}} - 1 \right) \frac{\Pi_t}{\bar{\Pi}} = \frac{\varphi \beta}{\eta_t} E_t \left\{ \frac{\tilde{\lambda}_{t+1}}{\tilde{\lambda}_t} \left(\frac{\Pi_{t+1}}{\bar{\Pi}} - 1 \right) \frac{\Pi_{t+1}}{\bar{\Pi}} \frac{\tilde{Y}_{t+1}}{\tilde{Y}_t} \right\} + (\epsilon - 1) \left[\frac{\epsilon}{\epsilon - 1} \frac{1}{\tilde{\lambda}_t} - 1 \right], \quad (14)$$

where $\tilde{\lambda}_t = \left[\tilde{C}_t - \tilde{\gamma} \tilde{C}_{t-1} \exp(-\varepsilon_{Z,t}) \right]^{-1}$ and $\tilde{\gamma} = \frac{\gamma}{G}$. These conditions along with the monetary policy rule and the stochastic processes for the three shocks must be satisfied in equilibrium. Equation (12) is the consumption Euler equation that jointly with the next equation, the aggregate resource constraint, constitute the basis for the aggregate demand relationship. Equation (14) is the nonlinear version of the New Keynesian Phillips curve that relates current inflation to expected future inflation and output.

3 Solution and Econometric Inference

Using the resource constraint to substitute out consumption, the model can be rewritten so that it has three endogenous state variables (\tilde{Y}_t , Π_t , and R_t^*) and three exogenous ones (η_t , $\varepsilon_{z,t}$, and $\varepsilon_{R,t}$). The

model is solved for a stationary solution (i.e., minimal rank solution) so that the model’s decision rules can be written as: $\mathbb{K}_t = h(\mathbb{K}_{t-1}, \tau_t)$, where $\mathbb{K}_{t-1} = (R_{t-1}^*, \Pi_{t-1}, \tilde{Y}_{t-1})$ and $\tau_t = (\eta_t, \varepsilon_{z,t}, \varepsilon_{R,t})$.

The model has two minimal rank solutions: one in which the unconditional mean of inflation is positive and another in which the unconditional mean of inflation is negative. The latter solution corresponds to the deflationary outcome studied by Benhabib, Schmitt-Grohé, and Uribe (2001). In the nonstochastic steady state associated with this equilibrium, the (net) nominal interest rate is zero and the (net) inflation rate is close to -2 percent. For our sample period, the average nominal interest rate is 4.5 percent and the average inflation rate is 2.4 percent. Moreover, even during the lower bound episode at the end of our sample, measures of expected inflation derived from financial markets and survey evidence, remained positive. Hence, we solve only for the minimal rank solution in which average inflation is positive and remains near $\bar{\Pi}$, the inflation target of the central bank.

The model is solved using a projection method, and the appendix discusses the methodology in detail, including how we solve only for the minimal rank solution in which average inflation is positive. In brief, the algorithm approximates the shock processes following Rouwenhorst (1995) and Kopecky and Suen (2010), who show that the Rouwenhorst (1995) method can match the conditional and unconditional mean and variance, and the first-order autocorrelation of any AR(1) process. The Rouwenhorst (1995) method is combined with approximating functions underlying the model’s decision rule with Chebychev polynomials and using collocation to determine the polynomial’s coefficients. We do not approximate $h(\mathbb{K}_{t-1}, \tau_t)$ directly with Chebychev polynomials, because these functions have a kink associated with the the interest-rate lower bound. Instead, we build on the ideas in Christiano and Fisher (2000) and approximate functions that are smoother and thus easier to approximate numerically while still allowing for a closed-form mapping into $h(\mathbb{K}_{t-1}, \tau_t)$.

Because we are estimating the model, it might be tempting to use a computationally-efficient solution algorithm that respects the nonlinearity in the Taylor rule but log-linearizes the remaining equilibrium conditions. This approach has been used by Christiano, Eichenbaum, and Rebelo (2011) and Erceg and Lindé (2012) among others. Unfortunately, we find that this approach performs poorly when applied to our model.⁸ As shown in the appendix, this solution algorithm can produce large quantitative differences in results from those arising from our approach along with relatively large Euler errors for empirically-realistic initial conditions. Accordingly, we choose to work with a projection

⁸ Other recent studies reach similar conclusions. See, for example, Nakata (2011) and Braun, Körber, and Waki (2012).

method building on the insights of Christiano and Fisher (2000), which is more accurate and still computationally efficient enough to use for estimation purposes. Another attractive feature of our projection method is that it takes into account the uncertainty about the likelihood that the economy will be at the lower bound in the economic decisions of households and firms.

We estimate the model using Bayesian methods. To do so we build on Fernandez-Villaverde and Rubio-Ramirez (2007), who first proposed using a particle filter within a Metropolis-Hastings algorithm to estimate nonlinear DSGE models.⁹ Because this approach is computationally burdensome, we follow the methodology developed in Smith (2011), who avoids having to compute the nonlinear model's likelihood function at every iteration of the Metropolis-Hastings algorithm through the use of a surrogate. This surrogate guides our sampling algorithm targeting the posterior distribution of the nonlinear model.

In this section we briefly outline the estimation procedure, and refer the reader to the technical appendix for details. After solving for the decision rule, $h(\mathbb{K}_{t-1}, \tau_t)$, our economic environment can be represented as a nonlinear state space model, where

$$\begin{aligned}\mathbb{Y}_t &= f_{\vartheta}(\mathbb{S}_t, \nu_t) \\ \mathbb{S}_t &= g_{\vartheta}(\mathbb{S}_{t-1}, \tau_t)\end{aligned}$$

In the above, \mathbb{Y}_t denotes the vector of observed variables which in our case includes data on the log-change in output ($\Delta y_t = \log \frac{Y_t}{Y_{t-1}}$), the logarithm of the gross inflation ($\pi_t = \log(\Pi_t)$), and the logarithm of the gross interest rate ($r_t = \log(R_t)$). The function $f_{\vartheta}(\mathbb{S}_t, \nu_t)$ describes how the variables in the economic model, \mathbb{S}_t are related to the data at each time period and the vectors \mathbb{S}_t and s_t are defined as: $\mathbb{S}_t = (s_t, s_{t-1})$ and $s_t = (\tilde{Y}_t, \tilde{C}_t, \Pi_t, \tilde{\lambda}_t, R_t, R_t^*, \eta_t, \varepsilon_{z,t}, \varepsilon_{R,t})$. The vector ν_t contains normally-distributed, *iid* measurement errors, one for each of in each of the observed variables: output growth, inflation, and the nominal interest rate; with standard deviations $\sigma_{\Delta y}$, σ_{π} , and σ_r , respectively.¹⁰ The function $\mathbb{S}_t = g_{\vartheta}(\mathbb{S}_{t-1}, \tau_t)$ defines the joint transition density of all the variables, while ϑ is a vector of parameters given by $\vartheta = (\beta, \gamma, \theta, \epsilon, \gamma_{\pi}, \gamma_y, \rho_R, \rho_{\eta}, \sigma_z, \sigma_R, \sigma_{\eta}, G, \bar{\Pi}, \sigma_{\Delta y}, \sigma_{\pi}, \sigma_r)$.

⁹See Andrieu, Doucet, and Holenstein (2010) for a formal justification for this and extensions to this class of algorithms, and Creal (2012) for a survey on applications of the particle filter in economics and finance.

¹⁰ Measurement error, besides being empirically realistic, facilitates the likelihood evaluation with the particle filter. As discussed in the appendix, it allows us to compute the density of the data given the state, a necessary step in the particle filter algorithm.

Our goal is to draw from the posterior distribution of parameters given the data $p(\vartheta|\mathbb{Y}_{1:T}) \propto p(\mathbb{Y}_{1:T}|\vartheta)p(\vartheta)$, where $p(\mathbb{Y}_{1:T}|\vartheta)$ is the likelihood function and $p(\vartheta)$ is a prior distribution of the parameters. We compute $p(\mathbb{Y}_{1:T}|\vartheta)$ using a particle filter (let \hat{p} denote a pdf that has been approximated by a particle filter) and embed it in a Metropolis-Hastings algorithm to draw from the posterior distribution of parameters. In light of the computational complexity involved in evaluating the policy functions and the likelihood function associated with the particle filter, we use a surrogate to aid in sampling from this distribution.

This surrogate requires the existence of some approximation to the posterior distribution, $\tilde{p}(\vartheta|\mathbb{Y}_{1:T})$ that can be evaluated quickly. We can use this approximation to pre-screen proposed parameter combinations in an otherwise standard Metropolis-Hastings algorithm. Let $\tilde{Q}(\vartheta, \cdot)$ be a proposal distribution with density $\tilde{q}(\vartheta, \vartheta')$, the algorithm is described in the following box.

Algorithm 1 Particle Marginal Metropolis-Hastings (PMMH) with Surrogate Transitions

```

set  $\vartheta^{(0)}$ 
for  $m = 1, \dots, L$  do
  set  $\vartheta = \vartheta^{(m-1)}$ 
  draw  $\tilde{\vartheta}' \sim \tilde{Q}(\vartheta, \cdot)$ 
  set  $\vartheta' = \tilde{\vartheta}'$  with probability  $\alpha_1(\vartheta, \tilde{\vartheta}') = \min \left\{ 1, \frac{\tilde{p}(\tilde{\vartheta}'|\mathbb{Y}_{1:T})\tilde{q}(\tilde{\vartheta}',\vartheta)}{\tilde{p}(\vartheta|\mathbb{Y}_{1:T})\tilde{q}(\vartheta,\tilde{\vartheta}')} \right\}$ , else set  $\vartheta' = \vartheta$ 
  if  $\vartheta' \neq \vartheta$  then
    set  $\vartheta^{(m)} = \vartheta'$  with probability  $\alpha_2(\vartheta, \vartheta') = \min \left\{ 1, \frac{\hat{p}(\vartheta'|\mathbb{Y}_{1:T})\tilde{p}(\vartheta|\mathbb{Y}_{1:T})}{\tilde{p}(\vartheta|\mathbb{Y}_{1:T})\hat{p}(\vartheta'|\mathbb{Y}_{1:T})} \right\}$ , else set  $\vartheta^{(m)} = \vartheta$ 
  else
    set  $\vartheta^{(m)} = \vartheta$ 
  end if
end for

```

This algorithm produces a Markov chain whose invariant distribution is $p(\vartheta|\mathbb{Y}_{1:T})$. The use of a surrogate allows us to avoid the expensive solution algorithm and particle filter evaluation at proposed parameter configurations $\tilde{\vartheta}'$ that are not likely to be accepted. We choose as our surrogate, $\tilde{p}(\vartheta|\mathbb{Y}_{1:T})$ a tempered posterior distribution created from log-linearizing our model. The linearized surrogate was chosen since the lower bound only binds for the last few years of our sample, so the resulting surrogate posterior (constructed from the linearized solution of the model) should be somewhat close to our posterior of interest (constructed from our nonlinear solution method). A second ‘accept/reject’ step corrects for the difference in these two distributions. We defer to the appendix many of the implementation details regarding the algorithm and the use of the particle filter to evaluate the likelihood

function. Also, see Smith (2011) for a further discussion of this method.

4 Estimation Results

4.1 Parameter Estimates

We estimate the model using U.S. data on output growth (Δy_t), inflation (π_t) and nominal interest rates (r_t) from 1983:Q1 through 2011:Q4. The focus on this sample helps abstract from changes in monetary policy regimes other than the lower bound episode at the end of the sample.¹¹ The data for the three-month T-bill rate and other series are all publicly available from the Federal Reserve Bank of St. Louis' FRED database.

The last three rows of Table 1 show the prior distributions of the structural parameters. These distributions are assumed to be independent across parameters, and their specification are based upon existing research. We do not estimate the average discount factor, β , which is set equal to 0.9987 and the elasticity of demand, ϵ , which is fixed at 6.

Columns two to four of Table 1 present the mean, standard deviation, and the 95 percent credible intervals from the posterior distributions of the parameters. The mean estimate of γ , is similar to our prior but the 95 percent credible interval—covering values between 0.35 to 0.59—is considerably tighter. To get a sense of how this estimate affects the dynamics of the model, it is useful to consider its interpretation from the linearized versions of equations (12)-(14), which are shown in the appendix. In the linearized version of the consumption Euler equation, $\gamma = 0.5$ implies that current output depends on lag-output with a coefficient of around $\frac{1}{3}$ and on one-quarter expected future output with a coefficient of about $\frac{2}{3}$, which is in line with the estimates of Smets and Wouters (2007) and Ireland (2011). In the linear version of the model, γ also governs the interest-rate elasticity of demand, $\frac{G-\gamma}{G+\gamma}$, whose mean value is slightly higher than $\frac{1}{3}$.

The posterior mean of the price adjustment cost parameter, φ , is very close to 95, which implies

¹¹ Output growth is measured by quarter-to-quarter changes in the log of real GDP (chained 2005 dollars, seasonally adjusted, converted to per capita terms using the civilian noninstitutional population ages 16 and over). The inflation rate is measured as the quarter-to-quarter change in the log of the GDP deflator, seasonally adjusted. Finally, the short-term nominal interest rate is measured by quarterly averages of daily readings on the three-month U.S. Treasury bill rate, converted from an annualized yield on a discount basis to a quarterly yield to maturity. A similar sample period has been used by Ireland (2011) and Aruoba, Bocola, and Schorfheide (2012). These papers use the three-month T-bill rate rather than the federal funds rate as the policy instrument though the two series track each other closely over our sample period. From 2009 onwards, after the FOMC established a target range from 0 to 25 basis points for the federal funds rate, the quarterly average federal funds rate and three-month T-bill rate have been within a few basis point of each other.

a linearized slope coefficient for the New Keynesian Phillips curve of 0.052. Comparing the linearized version of our New Keynesian Phillip curve with one with Calvo–Yun staggered-price setting, this estimate implies that firms change their price on average slightly more frequently than once a year. Accordingly, the mean estimate is in line with the microeconomic evidence on the frequency of price adjustment presented in Klenow and Malin (2011).

Our estimates imply considerable interest-rate smoothing, as embodied by the lagged coefficient in the rule, whose posterior mean is about 0.85. There is a significant, short-run interest-rate response to output growth, as the posterior mean of the coefficient γ_y is close to 0.25. The long-run response, $\gamma_y/(1 - \rho_R)$, is 1.77, which is in line with recent estimates by Aruoba, Bocola, and Schorfheide (2012) and Ireland (2011). The estimate of the posterior mean of the short-run reaction of the policy rate to deviations of inflation from the target level, γ_π , equals 0.79, which implies that the posterior mean of the long-run response, $\gamma_\pi/(1 - \rho_R)$ is about 5. This value is higher than estimates derived from DSGE models using Bayesian techniques, as our priors cover a wider range of permissible values than typically used. Still, the 95 percent credible interval for the long-run response of the policy rate to inflation deviations includes values as low as 2.5, which is more in line with these earlier estimates.

The estimate of the inflation target and technological growth rate are about 2.6 percent and 1.65 percent, respectively, on an annualized basis. The estimate for the inflation target is higher than the Federal Reserve’s current target, reflecting that the average inflation rate for our sample period is close to 2.5 percent. There is substantial persistence in the discount rate shock, as $\rho_\eta = 0.88$, and the standard deviation of innovations in technology are about six times larger than innovations in monetary policy.

The last three columns of Table 1 display the estimates for the measurement errors of the three observable variables. The posterior estimate of the standard deviation of the measurement error for the interest rate is low relative to the standard deviation of the measurement error either for output or inflation. We also computed the ratio of the measurement error variance to the total variance as $\sigma_j^2/var(j)$, for the appropriate variable $j \in \{\Delta y_t, \pi_t, r_t\}$. Based on a sample of 1000 draws from the posterior distribution, we find that this ratio is, on average, 2% for log GDP growth, 21% for log inflation and 1.5% for the log interest rate.¹²

¹² The ratio of the measurement error variance to the one step ahead forecast error variance is 2%, 33% and 13%, for GDP, inflation, and the interest rate, respectively.

4.2 Time Series Properties of the Model

Figure 1 compares the observed data on output growth, inflation, and the nominal interest rate with the smoothed estimates produced by the structural model. The figure also shows the 68 percent credible interval around these values.¹³

As shown in the top-left panel of the figure, the model is able to account for output growth well throughout the sample including the lower-bound period. In particular, the model produces the dramatic contraction in output growth that occurred in early 2009 as well as the subsequent rebound in growth. The model captures most of the low and medium frequency variation in quarterly inflation, displayed in the top-right panel. However, the high-frequency movements in inflation are partly explained by measurement error, which as discussed earlier accounts for about twenty percent of the volatility of the inflation series. For the recent recession, the model accounts for a substantial part of the fall and subsequent increase in inflation that occurred during that episode.¹⁴

The lower-left panel shows that the smoothed values for the nominal interest rate are close to the observed values and the lower-right panel displays the central bank’s notional or desired path for the nominal interest rate, which provides a measure of the severity of the lower-bound constraint on actual monetary policy. From 2009 onwards, the notional interest rate is well below zero, falling to minus 4 percent in the first half of 2009 and remaining well below zero until the end of our sample in 2011:Q4. Thus, our estimate of the notional rate suggests that the lower bound was an important factor contributing to the depth of the last recession. Later, in Section 5, we use the model to quantify the loss in output associated with this constraint.

Table 2 compares a variety of moments produced by the model to their empirical counterparts. The predictions of the model for the unconditional means and standard deviations of output growth and inflation are broadly consistent with the data. The model tends to understate the volatility of the nominal interest rate though the standard deviation of the observed interest rate remains near the upper limit of the model’s 95 percent credible interval.¹⁵

¹³ To construct these series, we proceed as follows: For each draw $\vartheta \sim p(\vartheta|\mathbb{Y}_{1:T})$, we sample from $p(\mathbb{S}_{1:T}|\mathbb{Y}_{1:T}, \vartheta)$ using the particle filter and report $f(\mathbb{S}_{1:T})$ for the appropriate function $f(\cdot)$. The credible intervals include both uncertainty surrounding ϑ as well as uncertainty surrounding $\mathbb{S}_{1:T}$. Similar results with tighter credible intervals are obtained when we report $E[f(\mathbb{S}_{1:T})|\mathbb{Y}_{1:T}, \vartheta]$ by averaging the smoothed series produced by the particle filter.

¹⁴ Some of the unexplained variation in inflation may reflect movements in oil prices. The price of crude oil fell sharply in 2008 from about 140 to 40 a barrel. This drop was accompanied by a nearly 50 percent fall in the energy price category of the CPI.

¹⁵ For the model, we report the mean estimate across parameter draws and take into account both parameter and

Table 2 also displays the autocorrelation for each of these three series. Output growth has an autocorrelation of nearly 0.5 over the sample period, which is just a bit above the model’s mean estimate. The autocorrelation of the observed nominal interest rate is only slightly higher than in the model, and the model is able to generate enough inflation persistence, even though its Phillips curve does not include lagged inflation term. The model’s success on these dimensions largely reflects the inclusion of habit persistence and the lagged interest rate in the policy rule. Notably, the presence of habits implies that the nonlinear Phillips curve depends on not only contemporaneous output but also lagged output, which helps generate persistent movements in inflation.¹⁶

The model is reasonably successful in accounting for the cross-correlations of the three variables. As in the data, the model generates positive correlations between the interest rate and inflation and the interest rate and output growth. The average correlation between output growth and inflation is about -0.3 in the model compared with essentially zero in the data. However, the 95 percent credible interval around this correlation is relatively large, encompassing slightly positive correlations.

4.3 The Propagation of Shocks at the Lower Bound

Before examining the shocks that drove the economy to their lower bound in late 2008, it is useful to first examine the effects of the two principal sources of fluctuations in the model: the productivity and discount rate shocks. Because the model is nonlinear, the effects of these shocks depend on the economy’s initial conditions, including the initial state for the exogenous shocks. To illustrate how the lower bound affects the propagation of these shocks, we consider two different sets of initial conditions: one in which the economy is far from a binding lower bound and another in which the constraint is binding. Although previous researchers have illustrated the effects of shocks at the lower bound by varying the initial conditions as we do here, they typically make assumptions about the initial state including the magnitudes of the shocks that put the interest rate at the lower bound. Instead, having estimated the model’s state including the shocks at each date, we are able to base the initial conditions for our impulse responses on empirically-realistic magnitudes for the shocks.

Figure 2 illustrates how the agents in the model expect the economy to evolve starting from two

sample uncertainty in constructing the confidence bands as follows. For each draw $\vartheta \sim p(\vartheta|\mathbb{Y}_{1:T})$, we simulate 10,000 samples each with 116 observations. We draw 1,000 times from our posterior distribution. The numbers in parentheses denote the 95% percent credible intervals.

¹⁶ This property is also a feature of the log-linearized version of the model shown in the appendix.

different initial conditions. In the first, the three lagged endogenous variables $(\tilde{Y}_{t-1}, \Pi_{t-1}, R_{t-1}^*)$ and the three exogenous shock values $(\eta_t, \varepsilon_{Z,t}, \varepsilon_{R,t})$ are set equal to their 2006:Q1 estimated values, which corresponds to an initial state in which output growth, inflation, and the nominal interest rate are relatively close to their unconditional means. In the simulation of this path, agents are assumed to know the initial state with certainty; subsequently, however, the shocks that hit the economy are uncertain and the figure plots the median path for each variable. For the path associated with the 2006:Q1 initial conditions (the dark solid line), the nominal interest rate is just above four percent and gradually rises up toward the steady state. Inflation at 3.5 percent initially is a bit high but in less than 2 years is close to the 2.5 percent target of the central bank. Output growth is somewhat higher than trend initially and then declines before returning to its unconditional mean growth rate.

The initial conditions of the economy are quite different in 2009:Q2. The lower right panel shows that the discount rate shock is about 1.5 percentage points below its mean zero level. The nominal interest rate is at the lower bound initially and its median value is expected to remain there for five quarters. Subsequently, the median path of the nominal interest rises but remains relatively low at the end of the simulation. Output growth is negative initially but is expected to rebound and turn positive after a couple of quarters. Inflation is around 1 percent initially and then gradually rises back to target.

A feature of the nonlinear model is that the response of inflation to marginal cost taking as given the expectation of future variables is non-constant; this effect is disregarded using the log-linearized equilibrium conditions. As shown in the bottom right panel of Figure 2, the slope of the Phillips curve is relatively low in 2009:Q1 when output is low as a result of the reduction in the discount rate. Because this shock reduces household demand, firms have less incentive to bear the cost of adjusting prices in the model and hence inflation becomes less responsive to changes in demand.

These different initial conditions can dramatically affect the propagation of the discount rate shock. The top panels of Figure 3 shows the effect of an unexpected increase in the discount rate in period 1 for the two different initial conditions. For each of variable shown in a panel of the figure, we report the median response relative to the baseline path illustrated in Figure 2 in which there is no unanticipated increase in the discount rate in period 1. For the shocked path, the discount rate is assumed to rise 35 quarterly basis points above baseline in period 1. Agents in the model then expected the shock to gradually revert back to baseline according to its estimated autocorrelation (i.e, the posterior mean of

ρ_η is 0.88). A positive discount rate shock, irrespective of whether it occurs in 2006:Q1 or 2009:Q2, stimulates current demand by the private sector at the expense of future spending, and as shown in the figure, this higher demand in turn translates into an increase in output and inflation.

If such a shock occurred in 2006:Q1, monetary policy is not constrained by the lower bound and reacts by raising the nominal interest rate more than one-for-one with the increase in inflation. Accordingly, the real interest rate (not shown) also rises, which has the effect of restraining the rise in output and inflation, helping the economy gradually return back to baseline. If such a shock occurred from 2009:Q2 onward, when the nominal interest rate is at the lower bound, the effects of the shock on output and inflation are substantially magnified.¹⁷ With monetary policy constrained by the lower bound, monetary policy is no longer as effective in offsetting the expansionary effects of the shock, therefore generating a larger increase in inflationary expectations and a lower real interest rate than in the scenario with more favorable initial conditions. Output rises about 1 percent above baseline, and inflation increases 1.3 percentage points, compared to 0.4 percent and 0.4 percentage point above baseline, respectively, in the scenario with more favorable initial conditions.

Although monetary policy is less effective in the scenario with unfavorable initial conditions, the estimated policy rule, by responding to the lagged notional rate, has the attractive property of offsetting the current expansion in demand by promising to raise future interest rates earlier and more than in the baseline. Accordingly, the median path of the nominal interest rate is at the lower bound for five quarters in the unshocked baseline, but only three quarters in the scenario with the increase in the discount rate. Subsequently, the median path of nominal interest rate rises sharply before gradually declining back to baseline.

Figure 3 demonstrates that the lower bound constraint can significantly affect the propagation of the discount rate shock. For the productivity shock, shown in the bottom four panels of Figure 3, this constraint also alters the dynamics of output and inflation, though less dramatically. As shown in the lower-left panel, an unanticipated increase in productivity increases the level of output about 1 percent above the baseline after 12 quarters regardless of the economy's initial conditions. Starting from the initial conditions in 2006:Q1, the increase in productivity initially boosts output 0.3 percent above baseline after which it monotonically rises towards its new higher level. Inflation drops about 30

¹⁷ This result is in line with a number of papers that have analyzed the effects of demand shocks (i.e., those that simultaneously boost output and inflation) at the lower bound. See, for example, Christiano, Eichenbaum, and Rebelo (2011) and Bodenstein, Erceg, and Guerrieri (2009).

basis points below baseline on impact and subsequently rises back toward its baseline value (of about 2.5 percent). Even with the favorable initial conditions, the nominal interest rate does not change much relative to baseline, as the drop in inflation and increase in output growth have largely offsetting effects. In particular, the estimated rule calls for only a small interest rate hike to counteract the large and persistent increase in output growth generated by the productivity shock.

With the desired interest rate not changing much when monetary policy is far from the lower bound constraint, imposing this constraint only has modest effects on output and inflation dynamics. When the economy starts from the unfavorable 2009:Q2 initial conditions, there is a larger increase in output and smaller decline in inflation than in the case with more favorable initial conditions. This amplification of the productivity shock on output reflects the gradual nature of the move to a tight monetary policy when the economy initially is at the lower bound.

5 What Accounts for the Great Recession?

The above impulse responses illustrate how the two main shocks in our analysis are propagated both in the region *away from* and *close to or at* the lower bound. This section builds on this analysis to examine the role of the estimated shocks in explaining the dynamics of output, inflation, and the nominal interest rate. We are particularly interested in understanding the role of these shocks in accounting for the economic slump associated with the 2007–2009 recession as well as for the interest rate’s long spell at the lower bound. Finally, we also use the estimated model to evaluate the contribution of the lower bound constraint to the most recent economic slump.

5.1 The Path of the Estimated Shocks

Figure 5 displays the smoothed estimates of the three shocks in the model: the discount rate, productivity, and the monetary policy shock. The shocks to the discount rate (η_t) tend to be high at the beginning of the sample, stabilize around their zero mean during most of the nineties—followed by a rise just before 2000 then a sharp fall before gradually reverting toward zero by 2006. As shown in the inner figure of the top panel, the discount rate shock then experiences a striking decline after 2006, reaching a trough around 2008:Q4 before gradually moving back up toward the end of the sample. Still, at the end of the sample, the shock implies that in 2011:Q4 the discount rate is more than 1

quarterly percentage point below its zero mean.

The estimated innovations to productivity ($\varepsilon_{Z,t}$) are depicted in the middle panel of Figure 5. Changes in productivity do not display much serial correlation over the sample period; however, the estimates imply that productivity was relatively low during the beginning of the Great Recession, suggesting that it may have contributed to the large, initial output contraction at the end of 2008. In 2010, productivity recovered from its very low level though remained relatively weak, on average, through the end of the sample period.¹⁸

The lower panel displays the innovations to the monetary policy rule, which are relatively small in comparison with the other two shocks.¹⁹ This result is consistent with the evidence in Christiano, Eichenbaum, and Evans (1999); however, it does not necessarily imply that monetary policy is unimportant, because the systematic part of the rule is a crucial determinant of the model's dynamics. Imposing the interest rate lower bound constraint on economic behavior greatly affects the pattern of policy shocks during the Great Recession. The inside figure in the lower panel shows that when the interest-rate lower bound is imposed, the monetary policy shocks are small and that policy is a bit stimulative at the onset of the recession. By contrast, Ireland (2011), who estimates a linearized model that does not impose the lower bound constraint, finds that a sequence of contractionary monetary policy shocks is necessary in order to match the observed interest rate trajectory during the Great Recession. Thus, misspecifying the model by ignoring the lower bound constraint might lead a researcher to the incorrect conclusion that the central bank chose to deviate from the systematic portion of their rule by surprising the public with unusually tight policy.

5.2 Shock Decomposition

Figure 6 shows how much of the model's fit for output growth, inflation, and nominal interest rates is attributable to individual shocks. More specifically, it displays the model's dynamics if only one of the three shocks were present during the Great Recession and compares this simulated path to the

¹⁸ In order to assess the plausibility of our estimated technology shocks, we compared them with measures in Fernald (2012), who uses a growth accounting methodology to estimate technological growth. Although his methodology in measuring productivity innovations is very different, the correlation between his measure with ours when adjusted for variable factor utilization is 0.49 and 0.69 when unadjusted.

¹⁹ Monetary policy shocks are still identified at the lower bound, because these shocks can persistently lower the notional interest rate. As a result, agents anticipate that the actual nominal rate will be at the lower bound for longer, an expectation that affects current outcomes.

smoothed values shown in Figure 1, which were generated using all three shocks.²⁰ The upper-left panel of the figure shows that the large contraction in output growth that occurred at the end of 2008 was attributable to both the fall in productivity and the discount rate, as either of these two shocks alone would have induced the level of output to fall in 2008:Q4. While both of these shocks contributed to slow output growth from 2009 onwards, the model ascribes a relatively larger role to the productivity shocks.

The discount rate shocks, however, appear to be relatively more important in explaining the low inflation in 2009 and 2010. Despite the large decline in demand induced by this shock, the fall in inflation is relatively modest and the economy never experiences deflation. This mild disinflation reflects in part the upward pressure on marginal cost induced by the decline in productivity in late 2008 and 2009. In addition, as shown in Figure 2, the slope of the Phillips curve flattens out, dampening the response of inflation to the large fall in demand induced by the discount rate shock.

The decline in the discount rate is also important in accounting for the economy’s spell at the lower bound. By reducing both output growth and inflation, this shock pushes the notional interest rate well below zero, causing the interest rate to hit and then stay at the lower bound throughout the episode.

5.3 The Contribution of the Zero Lower Bound to the Great Recession

How much did the interest-rate lower bound contribute to the economic slump during the Great Recession? To address this question, we use our model to compare its estimated outcomes to the outcomes from a hypothetical scenario in which monetary policy is free to adjust the nominal interest rate in an unconstrained manner. Figure 7 reports the observed data on output, inflation, and the nominal rate, the outcomes for these series from the estimated (constrained) model, and the outcomes implied by a hypothetical scenario in which monetary policy is able to make the policy rate negative.²¹ If policy could have acted in an unconstrained fashion, the policy rule would have called for a negative nominal interest rate from 2009 to the end of the sample period. In 2009, this hypothetical rate would have been close to -4 percent throughout 2009 and below -1 percent at the end of the sample in 2011:Q4. The

²⁰ We also considered an alternative decomposition in which the dynamics were influenced by two of the three, which yielded broadly similar conclusions. We compute the counterfactual with only one shock present as follows: Starting in 2007:Q4, we take the estimated state (shown in Figure 1) as a starting value, and simulate the economy forward feeding in one the smoothed values of one shock processes, say $\varepsilon_{\eta,t}$, assuming $\varepsilon_{Z,t} = \varepsilon_{R,t} = 0$. Analogous exercises are performed to plot the ‘Tech Only’ and ‘Monetary Only’ series.

²¹ The hypothetical scenario uses the estimated initial conditions and time series for the shocks from the version of the model in which the constraint is imposed. These values are then used to simulate the unconstrained version of the model.

95 percent credible interval around these estimates indicates that there was only a small probability that the hypothetical nominal rate would have turned positive during this period.

If monetary policy could have cut the nominal interest rate this aggressively, it would have helped offset the contractionary effects of the productivity and discount rate shocks and thus output and inflation would not have fallen as dramatically during the recession. The upper-right panel shows that output is more than 1 percent lower, on average, over the 2009–2011 period in the estimated, constrained version of the model relative to the hypothetical scenario.²² Moreover, around 20 percent of the initial fall in output in early 2009 is due to the lower bound constraint. Inflation, displayed in the upper-right panel, is further below the central bank’s inflation target throughout the 2009–2011 period and is about 0.5 percentage point lower, on average, over this period in the constrained model relative to the unconstrained model. Accordingly, our estimates suggest that the interest-rate lower bound was a significant constraint on monetary policy that helped exacerbate the recession and inhibit the recovery.

6 Lower Bound Episodes

This section examines the model’s estimates of the probability of the interest rate reaching the lower bound and the average duration of a lower bound spell. It is useful first to provide some context from the data. For our sample period from 1983:Q1–2011:Q4, there is one realization of a lower bound episode in which the nominal interest rate is effectively at the lower bound. The episode has lasted for 12 quarters to the end of the sample in 2011:Q4, so that the duration of the episode is right-censored. While these numbers are useful as an *ex-post* description of this episode, below we provide a more complete characterization by examining the evolution of private sector’s expectations of the duration of the lower bound spell. As documented below, measures of private sector expectations of the duration, both at the beginning and middle of the spell, were for spells to last only 3 to 4 quarters.

²² It may be surprising that there is such a persistent difference in the two scenarios in light of the fact that the only source of difference is the monetary policy reaction function. After all, monetary policy in the long run is neutral in the model. However, the estimates of the shock innovations imply that the economy was continually buffeted by shocks throughout this episode so that the economy is still far from converging back to its ergodic steady state.

6.1 The Expected Path of the Nominal Interest Rates

To illustrate this, the top panels of Figure 8 display investor expectations for the path of the federal funds rate using data from Eurodollar quotes and implied three-month forward rate swaps for two different dates.²³ The upper left panel shows that at the beginning of the lower bound episode in 2009:Q1, the median forecast (the solid yellow line) by financial market participants was for the federal funds rate to remain below 25 basis points through the third quarter of 2009 before rising gradually to about 2.5 percent in 2012.²⁴ As indicated by the dark and light shaded regions, which represent the 70 and 90 percent confidence intervals respectively, there is considerable uncertainty around these forecasts at longer horizons. Even taking into account this uncertainty, however most financial participants in 2009:Q1 expected the federal funds rate to remain below 25 basis points for only a few quarters.

The upper right panel shows that the distribution for the expected federal funds rate had shifted downward by 2010:Q2. Financial market participants in 2010:Q2 were expecting, on average, that the federal funds would remain below 25 basis points for four quarters, compared with three quarters in 2009:Q1. In addition, the distribution for the expected federal funds rate one to two years in the future is lower in 2010:Q2 than in 2009:Q1.

The bottom panels of Figure 8 display the expected path for the nominal interest rate in 2009:Q1 and 2010:Q2 using 3-month Treasury yield forecasts from the Blue Chip Economic Indicators.²⁵ Private sector forecasts, on average, expected the nominal rate to remain below 25 basis points for about 3 quarters in both 2009:Q1 and 2010:Q2. Moreover, the expected path for the nominal rate rises a bit faster and to a higher level than as implied by financial market data. In 2009:Q1, for example, the nominal rate is expected to reach 4 percent by the end of 2014 compared to 2.5 percent based on the expectations of financial market participants.

Figure 8 also shows the projected paths for the federal funds rate implied by our model. In 2009:Q1, the model predicts a median path in which the nominal interest rate stays at the lower bound for four

²³ See Jarrow, Li, and Zhao (2007) for a discussion of how the distribution for the expected federal funds rate path is computed from financial market quotes.

²⁴ For 2009:Q1, we used financial market quotes from March 18, 2009, and for 2010:Q2, we used quotes from June 16, 2010.

²⁵ Individual market expectations are reported monthly by survey participants for the current quarter to five quarters ahead, with annual estimates collected semi-annually for up to five years ahead. For 2009:Q1, we use the March 10, 2009 release and for 2010:Q2, we used the average of the reported consensus estimates from the March 10, 2010 and October 10, 2010 releases. Confidence bounds represent the mean of the 10 highest and lowest observations in the sample of 46 market participants surveyed in the Blue Chip release. A cubic spline was used to interpolate the quarterly paths from the annual observations.

consecutive quarters. Thereafter, the interest rate is expected to rise gradually, reaching 4 percent at the end of 2014. As shown by the dashed lines, there is substantial uncertainty around the model’s projections, both for the duration of the lower bound spell and for the value of the interest rate in early 2015. Similar to both financial market participants and private sector forecasters, the model’s median duration is four quarters in 2009:Q1. Although the projected path of interest rates rises faster from 2010 onward than the path implied by financial data, it is remarkably similar to the projected path of private sector forecasters.

The lower right panel shows that in 2010:Q2 the model’s path is largely in line with the expected path of Blue-Chip forecasters, whose projections take into account the unconventional policies implemented between 2009:Q1 and 2010:Q2. Although the model’s expected duration is only two additional quarters in 2010:Q2 compared with the four-quarter projection of financial market participants, the model’s 68 percent confidence bands (the dotted lines) include a duration of 6 quarters. Accordingly, the model captures the downside risk associated with staying at the effective lower bound implicit in financial market quotes.

In summary, the model has reasonable implications for the expected duration and path of the nominal interest rate during the lower bound spell that occurred in our sample. Although the model incorporates a forward guidance channel through the expected path implied by the interest-rate rule, it does not take into consideration the balance-sheet policies undertaken by the Federal Reserve in recent years. Despite this omission, the model still generates an expected interest rate path that is reasonably similar to those of financial market participants and private sector forecasters.

6.2 The Probability of Being at the Lower Bound

The top panel of Figure 9 displays the cumulative distribution function of the probability of being at the zero lower bound implied by the model’s estimates. The dark line shows the cumulative distribution function in which the only source of variation in this probability is the uncertainty coming from the posterior estimates of the model’s parameters.²⁶ We call this the *population* estimate of the lower bound probability. As implied by the population histogram, the economy is at the zero lower bound,

²⁶ The cumulative distribution function are constructed from histograms in which we used 100 draws from the posterior distribution of the parameters, $\vartheta \sim p(\vartheta|Y_{1:T})$. For each draw, we simulate the economy for 1,000,000 time periods and compute the fraction of time the economy is constrained by the lower bound to get the population estimate. To compute the (small) sample estimate, we break this long sample into bins of 116 time periods, compute the fraction of time that the economy is at the zero lower bound, and use the resulting histogram to estimate the sample distribution.

on average, about 3 percent of the time. However, the estimates of this probability are disperse, ranging from close to 0 to above 5 percent and having a standard deviation of close to 1 percent. The distribution has fat tails and the middle panel zooms in on the right tail. As indicated there, our estimates suggest that 2.5 percent of the posterior draws produce an economy that is at the lower bound 5 percent of the time or longer. In contrast, for our empirical sample, the interest rate has been at the lower bound for 12 of the 116 quarters, about 10 percent of the time.

A possible interpretation of this discrepancy is that the model can not generate a fraction of time spent at the lower bound that matches our sample of data. This interpretation is not appropriate, however. Our model suggests that it is not possible to reliably estimate the probability of being at the lower bound in a small sample. To illustrate this point, the dashed line in the upper panel shows the cumulative distribution function derived from the model’s estimates using samples of length $T = 116$. In this case, the average probability of being at the lower bound is still 3 percent; however, the sample distribution displays more dispersion, as the right-tail spreads out even more (see the bottom panel of figure 9). Here, 14 percent of our samples reached the lower bound for at least 8 of 116 quarters. As indicated in the upper panel, almost 50 percent of the samples generated by the model never even hit the interest-rate lower bound. Hence, a situation in which no lower bound episodes are observed in 116 quarters of data is fairly likely. The interest rate reaches the lower bound for 12 or more quarters in about 5 percent of the samples, and 0.05 percent of the samples reached the lower bound for more than 35 of the 116 quarters.

6.3 The Duration of Lower Bound Spells

The top panel of Figure 10 displays the (population) cumulative distribution function of the duration of a lower-bound spell.²⁷ The average duration for a lower bound spell is just over three quarters and the median is two. The distribution for the duration of a spell is skewed to the right and also has a long right tail (shown in the bottom panel). Spells with durations of eight quarters or longer occur account for about 9 percent of the total number of lower bounds spells and those with durations of twelve quarters or longer account for 2.8 percent of the total. Thus, the current episode, with a duration of at least twelve quarters, occurs relatively infrequently in the model, and from the perspective of

²⁷ The (population) cumulative distribution function is constructed from a histogram in which we used 1000 draws from the posterior distribution of the parameters, $\vartheta \sim p(\vartheta | \mathbb{Y}_{1:T})$. For each draw, we simulated the economy for 1,000,000 time periods and computed the duration of each lower bound spell.

households and firms in the model, would be difficult to predict *ex ante*. This finding is consistent with the evidence obtained from financial markets and private sector forecasts, which for the most part did not foresee such a protracted episode.

Figure 11 shows the dynamic paths of the median responses of the economy's variables in a long duration spell (defined as spells whose duration is twelve quarters or longer) and the median responses of short duration spells (defined as spells whose duration is less than twelve quarters). For purposes of comparison, the figure also plots the (nonstochastic) steady state growth path for output, the level of the inflation target, and the steady state nominal interest rate. For both types of spells, the economy starts from the 2008:Q4 initial conditions; these conditions include the smoothed values of the shocks in that quarter (shown as the first quarter in the lower panels of the figure). With the economy starting from the same unfavorable position in which both the productivity and discount rate shocks are very low, the responses of the variables in the first period in both scenarios are the same. In a short spell, the unfavorable initial positions of the shocks are relatively temporary. The productivity innovation ($\varepsilon_{Z,t}$) immediately returns to its mean value of zero after one period while the discount factor shock (η_t) gradually returns back to its mean zero according to $\rho_\eta = 0.88$, the posterior mean value. With the shocks returning back to baseline, inflation converges back to its steady-state level after ten quarters. In addition, the nominal rate departs from the lower bound after four quarters and only slowly returns back to its steady state level, reflecting the high degree of inertia in the rule (i.e., $\rho_R = 0.86$).

In a long spell, the unfavorable circumstances are much more persistent. The discount rate shock stays at a very low level and only gradually begins to return its mean level after 12 quarters. Accordingly, output falls further below trend before beginning to improve. Inflation displays a similar pattern, declining to just below 1 percent after two years and then gradually rising back to the central bank's target. The nominal interest also remains at the lower bound for 14 quarters and remains well below its unshocked level five years after the start of the simulation.

Note that many of the characteristics of the median response of the long duration simulation resemble the empirical lower bound episode we discussed earlier. In this episode, output growth remained persistently weak, and though inflation falls, there is not a prolonged spell of deflation.

6.4 Explaining the Probability and Duration of Lower Bound Spells

The preceding discussion underscores the important role of the demand or discount rate shock in bringing about a lower bound episode. We turn now to the issue of how other structural features of the economy affect the probability of reaching the lower bound and the duration of an episode. Figure 12 shows scatter plots of how key parameters affect the probability and duration of a spell.²⁸ The first row of the panels display the relationship between the persistence of the discount rate shock and three statistics about the lower bound: the probability of the interest rate being at the lower bound, the average duration of a lower bound spell, and duration in the tail of the distribution (defined as the 99.5th percentile). The frequency and duration of spells tend to increase for economies in which discount factor shocks are more persistent. The univariate regression coefficient is positive and statistically significant at the 95 percent confidence level.

Monetary policy rule parameters can also be important determinants of lower bound spells. The second row shows that the greater the inertia in the rule, as measured by the lagged interest rate coefficient (ρ_R), the higher the probability of a lower bound spell and the greater the duration of the spell. Although inertia in the rule tends to make a lower bound spell more likely, this does not necessarily imply inertia is an undesirable feature of monetary policy. In fact, placing a greater weight on the lagged notional rate, the outcomes for inflation and activity in a lower-bound spell results in better economic outcomes than a rule with less inertia.

The average growth rate of productivity, G , is a key determinant of the model's average nominal interest rate and thus the probability and duration of a lower bound episode. The lower panels of Figure 12 demonstrate that model economies with a lower average growth rate are more susceptible to more and longer lasting lower bound spells.

7 Conclusions

In this paper, we estimated a nonlinear DSGE model in which the interest-rate lower bound is occasionally binding. This allowed us to quantify the size and nature of the disturbances that pushed the U.S. economy to the lower bound in late 2008 as well as conclude that the lower bound was a significant

²⁸ The scatter plots are constructed from 1000 draws from the posterior distribution of the parameters, $\vartheta \sim p(\vartheta | \mathbb{Y}_{1:T})$. For each draw, we simulated the economy for 1,000,000 time periods and computed the number of periods at the bound and the duration of each spell.

factor in exacerbating the economic slump during that period. We also found that the New Keynesian model is capable of generating long-lasting lower-bound spells that resemble the observed U.S. episode and yields predictions consistent with private sector forecasts regarding the expected duration of the episode.

Researchers interested in examining the effects of alternative policies at the lower bound often need to calibrate their models with reasonable parameters but also reasonably-sized shocks. The exercise conducted here should be especially beneficial to these researchers, because our parameter estimates and even more so our shock estimates can be used to create realistic initial conditions from which to conduct such policy experiments. More broadly, we have demonstrated that it is possible to solve a nonlinear model using projections methods and then estimate the model using Bayesian techniques. This approach is likely to prove fruitful for other applications in which occasionally binding constraints have important economic consequences.

References

- An, S. and F. Schorfheide (2007). Bayesian analysis of DSGE models. *Econometric Reviews* 26, 113–172.
- Andrieu, C., A. Doucet, and R. Holenstein (2010). Particle markov chain monte carlo with discussion. *Journal of Royal Statistical Society Series B* 72, 269–342.
- Aruoba, S. B., L. Bocola, and F. Schorfheide (2012). A new class of nonlinear time series models for the evaluation of DSGE models. University of Maryland, manuscript.
- Aruoba, S. B. and F. Schorfheide (2012). Macroeconomic dynamics near the ZLB: A tale of two equilibria. University of Pennsylvania, manuscript.
- Basu, S. and B. Bundick (2012). Uncertainty shocks in a model of effective demand. NBER Working Paper 18420.
- Benhabib, J., S. Schmitt-Grohé, and M. Uribe (2001). The perils of taylor rules. *Journal of Economic Theory* 96, 40–69.
- Bodenstein, M., C. J. Erceg, and L. Guerrieri (2009). The effects of foreign shocks when interest rates are at zero. International Finance Discussion Paper 1009.
- Bodenstein, M., L. Guerrieri, and C. J. Gust (2012). Oil shocks and the zero bound on nominal interest rates. *Journal of International Money and Finance*. Forthcoming.
- Braun, R. A., L. M. Körber, and Y. Waki (2012). Some unpleasant properties of log-linearized solutions when the nominal interest rate is zero. Federal Reserve Bank of Atlanta, WP 2012-5a.
- Christiano, L., M. Eichenbaum, and S. Rebelo (2011). When is the government spending multiplier large? *Journal of Political Economy* 119, 78–121.
- Christiano, L. J., M. Eichenbaum, and C. L. Evans (1999). Monetary policy shocks: What have we learned and to what end? In J. Taylor and M. Woodford (Eds.), *Handbook of Macroeconomics Vol.1*, pp. 65–148. Elsevier.
- Christiano, L. J., M. Eichenbaum, and C. L. Evans (2005). Nominal rigidities and the dynamic effects of a shock to monetary policy. *Journal of Political Economy* 113, 1–45.
- Christiano, L. J. and J. D. Fisher (2000). Algorithms for solving dynamic models with occasionally binding constraints. *Journal of Economic Dynamics and Control* 24, 1179–1232.
- Chung, H., J.-P. Laforte, D. Reifschneider, and J. Williams (2012). Have we underestimated the likelihood and severity of zero lower bound events? *Journal of Money, Credit and Banking* 44, 47–82.
- Coenen, G., A. Orphanides, and V. Wieland (2004). Price stability and monetary policy effectiveness when nominal interest rates are bounded at zero. *Advances in Macroeconomics* 4, 1187–1187.
- Creal, D. (2012). A survey of sequential Monte Carlo methods for economics and finance. *Econometric Reviews* 31, 245–296.
- Eggertsson, G. and M. Woodford (2003). The zero bound on interest rates and optimal monetary policy. *Brookings Papers on Economic Activity* 1, 139–211.
- Erceg, C. J. and J. Lindé (2012). Is there a fiscal free lunch in a liquidity trap. *Journal of European Economic Association*. Forthcoming.

- Fernald, J. (2012). Productivity and potential output before, during, and after the great recession. Federal Reserve Bank of San Francisco, manuscript.
- Fernandez-Villaverde, J., G. Gordon, P. Guerron-Quintana, and J. Rubio-Ramirez (2012). Nonlinear adventures at the zero lower bound. National Bureau of Economic Research Working Paper 18058.
- Fernandez-Villaverde, J. and J. Rubio-Ramirez (2007). Estimating macroeconomic models: A likelihood approach. *Review of Economic Studies* 74, 1059–1087.
- Hall, R. E. (2011). The high sensitivity of economic activity to financial frictions. *The Economic Journal* 121, 351–378.
- Ireland, P. N. (2011). A new keynesian perspective on the great recession. *Journal of Money, Credit, and Banking* 43, 31–54.
- Jarrow, R., H. Li, and F. Zhao (2007). Interest rate caps ‘smile’ too! but can the libor market models capture it? *Journal of Finance* 62, 345–382.
- Klenow, P. and B. Malin (2011). Microeconomic evidence on price-setting. In B. Friedman and M. Woodford (Eds.), *Handbook of Monetary Economics Vol. 3A*, pp. 231–284. Elsevier.
- Kopecky, K. A. and R. M. H. Suen (2010). Finite state markov-chain approximations to highly persistent processes. *Review of Economic Dynamics* 13, 701–714.
- Nakata, T. (2011). Uncertainty at the zero lower bound. New York University, manuscript.
- Rotemberg, J. (1982). Sticky prices in the United States. *Journal of Political Economy* 90, 1187–1211.
- Rouwenhorst, K. (1995). Asset pricing implications of equilibrium business cycle models. In T. Cooley (Ed.), *Frontiers of Business Cycle Research*, pp. 294–330. Princeton University Press.
- Smets, F. and R. Wouters (2007). Shocks and frictions in the U.S. business cycles: A bayesian DSGE approach. *American Economic Review* 97, 586–606.
- Smith, M. (2011). Estimating nonlinear economic models using surrogate transitions. Federal Reserve Board, manuscript.

Table 1: Estimation Results

parameter	mean	stdev	0.025	0.975	prior type	prior mean	prior stdev
γ	0.46629	0.05990	0.35116	0.59479	Beta	0.50000	0.22373
φ	94.23848	14.95835	66.41825	124.96302	Gamma	85.00000	15.00000
γ_π	0.79127	0.11427	0.58608	1.03796	Normal	0.00000	1.00000
γ_y	0.25475	0.04955	0.16604	0.36333	Normal	0.00000	1.00000
ρ_R	0.85622	0.03549	0.78340	0.92342	Beta	0.50000	0.27929
ρ_η	0.88018	0.01766	0.83982	0.90892	Beta	0.50000	0.27929
σ_z	0.01323	0.00175	0.01026	0.01737	InvGamma1	0.01000	0.01000
σ_R	0.00210	0.00024	0.00170	0.00263	InvGamma1	0.01000	0.01000
σ_η	0.00252	0.00031	0.00200	0.00321	InvGamma1	0.01000	0.01000
G	1.00413	0.00057	1.00309	1.00532	Normal	1.00433	0.00100
$\bar{\Pi}$	1.00656	0.00032	1.00594	1.00721	Normal	1.00607	0.00100
$\sigma_{\Delta y}$	0.00101	0.00010	0.00084	0.00123	InvGamma1	0.00100	0.00050
$\sigma_{\Delta\pi}$	0.00117	0.00010	0.00099	0.00139	InvGamma1	0.00100	0.00050
σ_r	0.00081	0.00006	0.00071	0.00094	InvGamma1	0.00100	0.00050

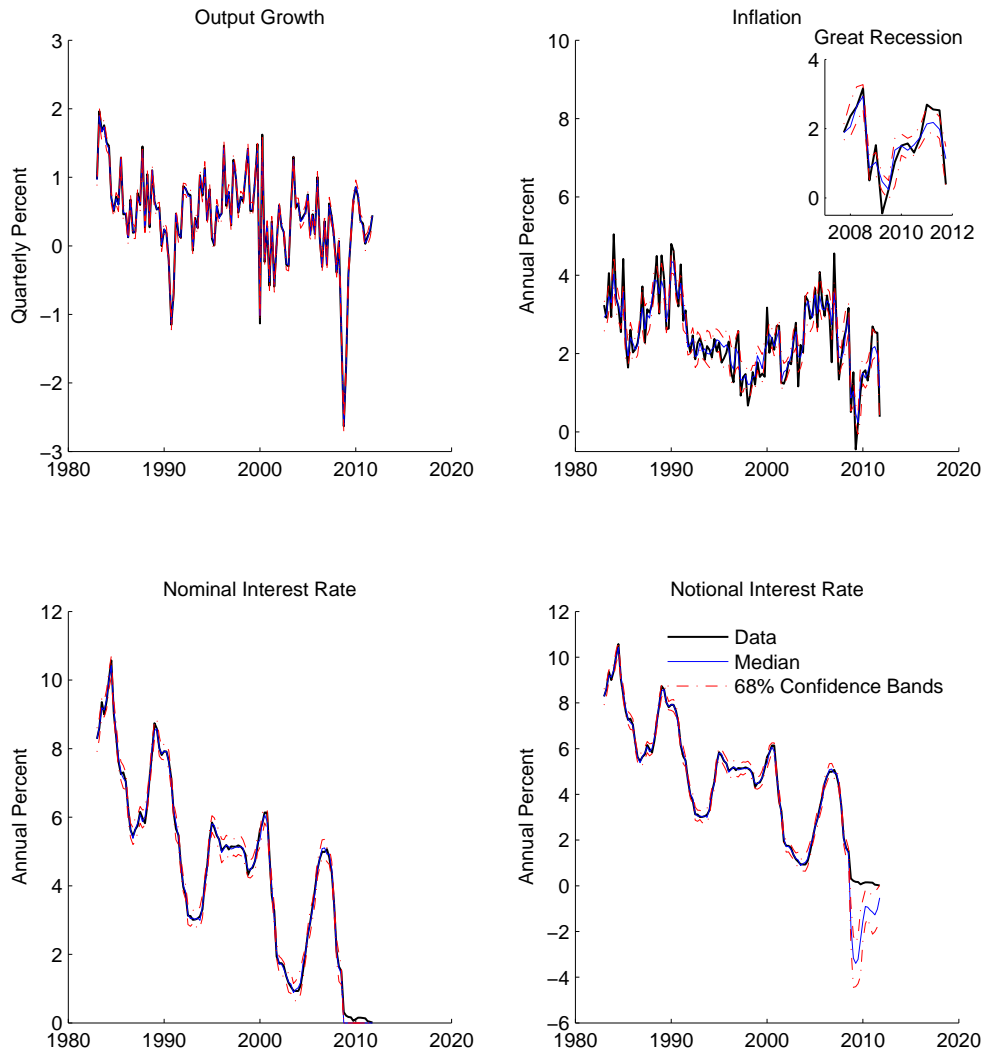
Note: The Markov chain was run for 200,000 iterations and the particle filter used 240,000 particles. The overall acceptance rate was 34 percent and approximately 30 percent of the draws were rejected by the surrogate criteria α_1 . No burn-in for the chain was used as a significant amount of tuning went into the algorithm. The tempered surrogate was constructed using the linearized equations and either the same or more diffuse priors. The surrogate was tempered by a factor of 5. We take every 200th draw to leave 1000 draws to perform inference in the remaining sections of the paper.

Table 2: Unconditional Moments: Data and Model

		Data	Model		Data	Model
$x = \Delta y$	\bar{x}	1.72	1.63 (0.51, 2.70)	$corr(\Delta y, \Delta y_{-1})$	0.47	0.46 (0.24, 0.66)
	σ_x	2.72	2.71 (2.13, 3.40)	$corr(\pi, \pi_{-1})$	0.57	0.70 (0.53, 0.82)
$x = \pi$	\bar{x}	2.42	2.57 (2.05, 3.07)	$corr(r, r_{-1})$	0.98	0.89 (0.80, 0.96)
	σ_x	1.03	0.90 (0.65, 1.22)	$corr(\Delta y, \pi)$	0.03	-0.30 (-0.61, 0.04)
$x = r$	\bar{x}	4.49	4.62 (3.07, 6.17)	$corr(\Delta y, r)$	0.33	0.05 (-0.25, 0.35)
	σ_x	2.67	1.82 (1.18, 2.60)	$corr(\pi, r)$	0.50	0.27 (-0.15, 0.61)

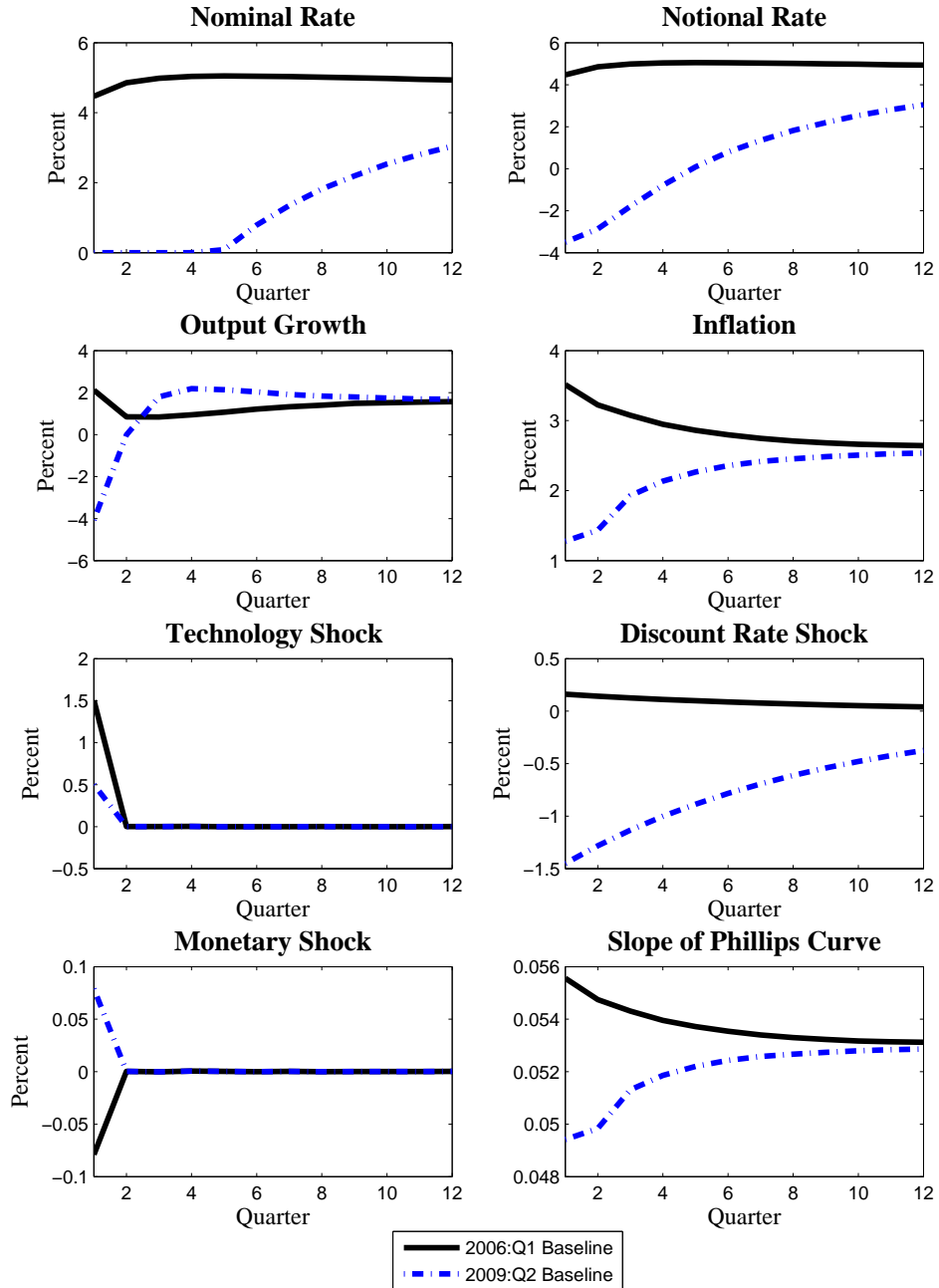
Note: For each draw $\vartheta \sim p(\vartheta|\mathbb{Y}_{1:T})$, we simulate 10,000 samples each with 116 observations. We draw 1,000 times from our posterior distribution. The numbers in parentheses denote the 95% percent credible intervals.

Figure 1: Smoothed Estimates of Model Objects



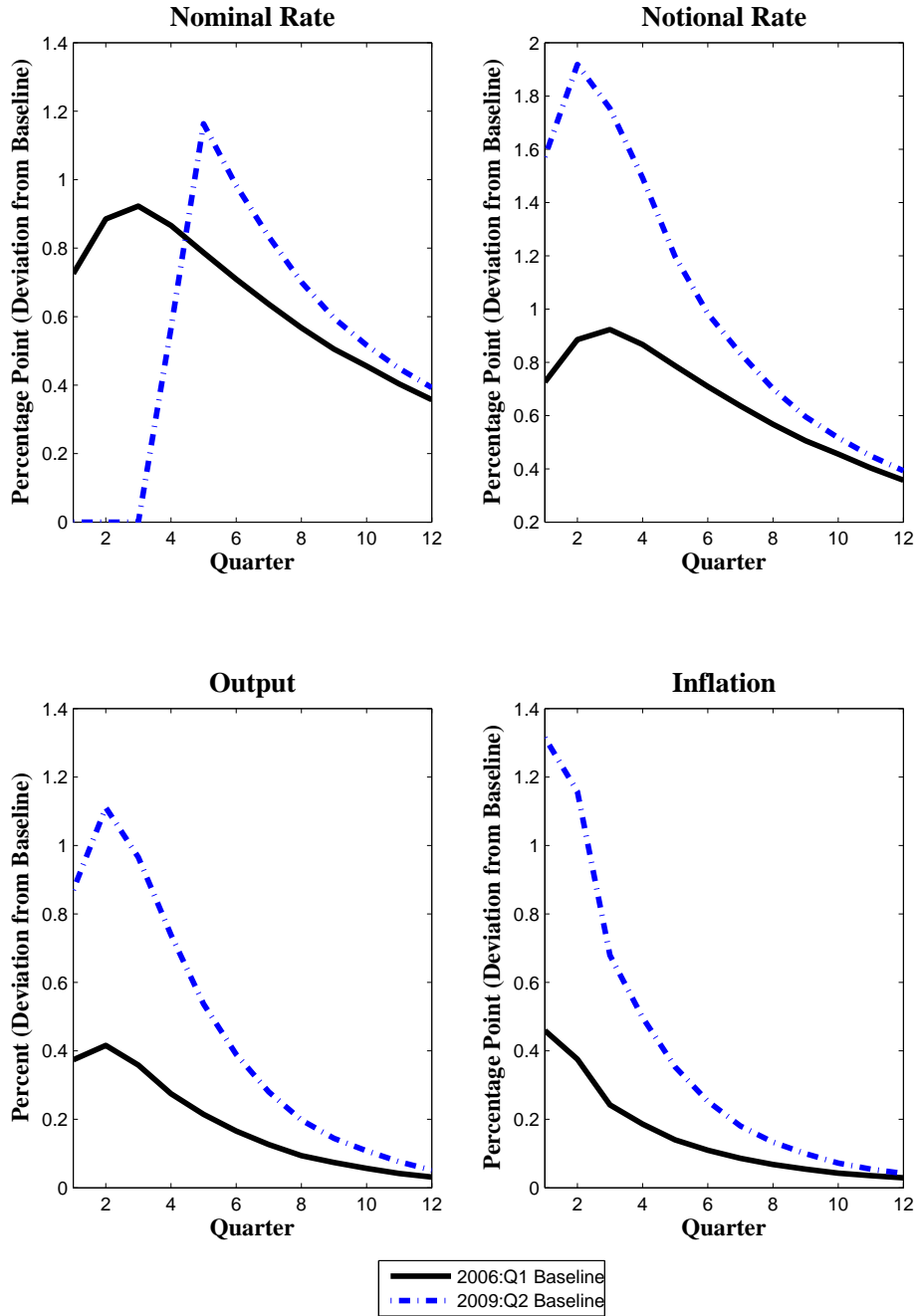
Note: For each draw $\vartheta \sim p(\vartheta|Y_{1:T})$, we sample once from $p(S_{1:T}|Y_{1:T}, \vartheta)$ using the particle filter and report $f(S_{1:T})$ for the appropriate function $f(\cdot)$. We draw 1000 times from our posterior distribution.

Figure 2: The Dynamic Paths of Alternative Initial Conditions



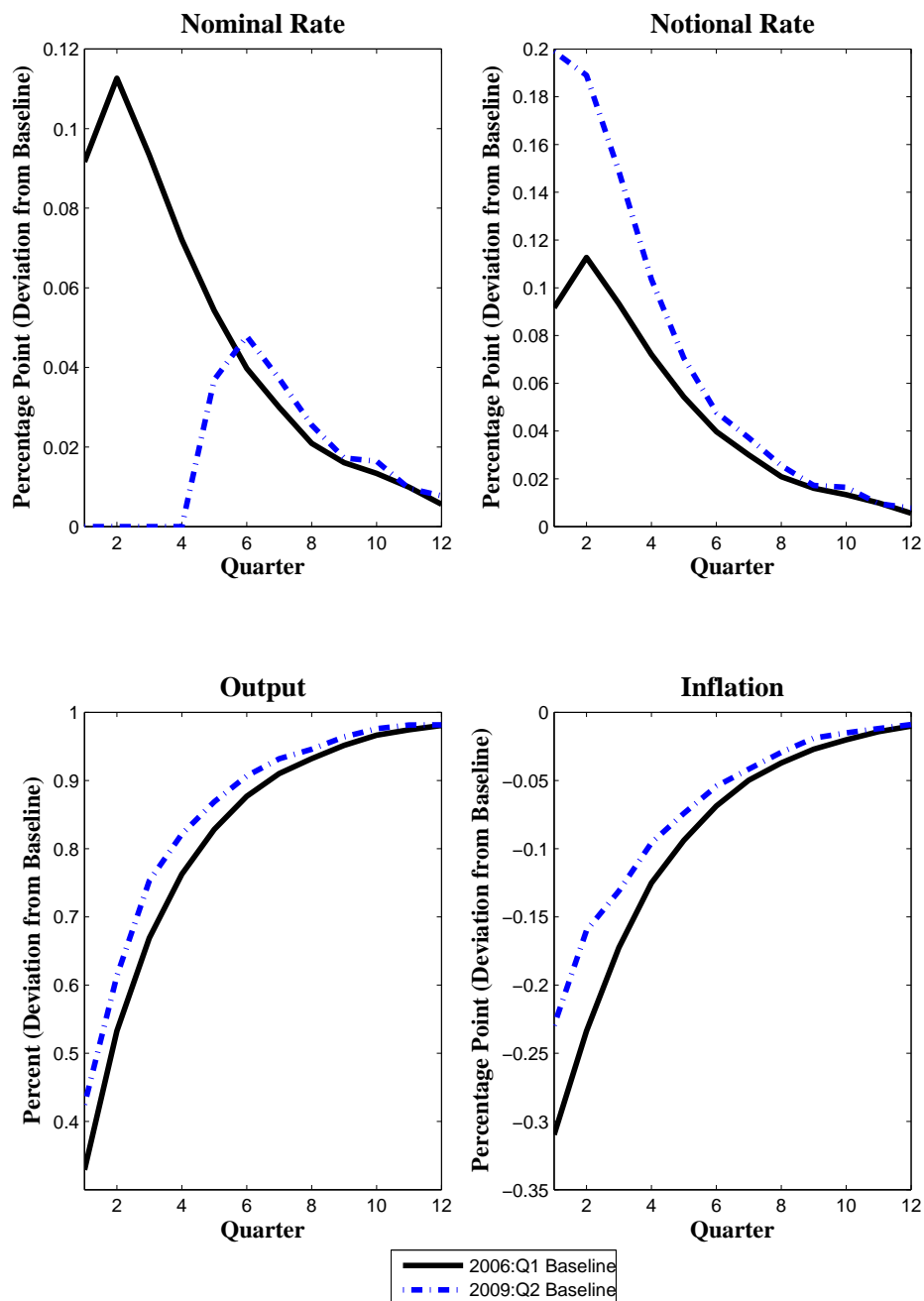
Note: The model responses are computed as follows. We use the posterior means of the parameter values, and the mean estimate of the state as initial conditions for each baseline scenario. We then simulate 1,000,000 paths and report the median value across these paths for each variable in each period.

Figure 3: The Effects of a Discount Rate Shock



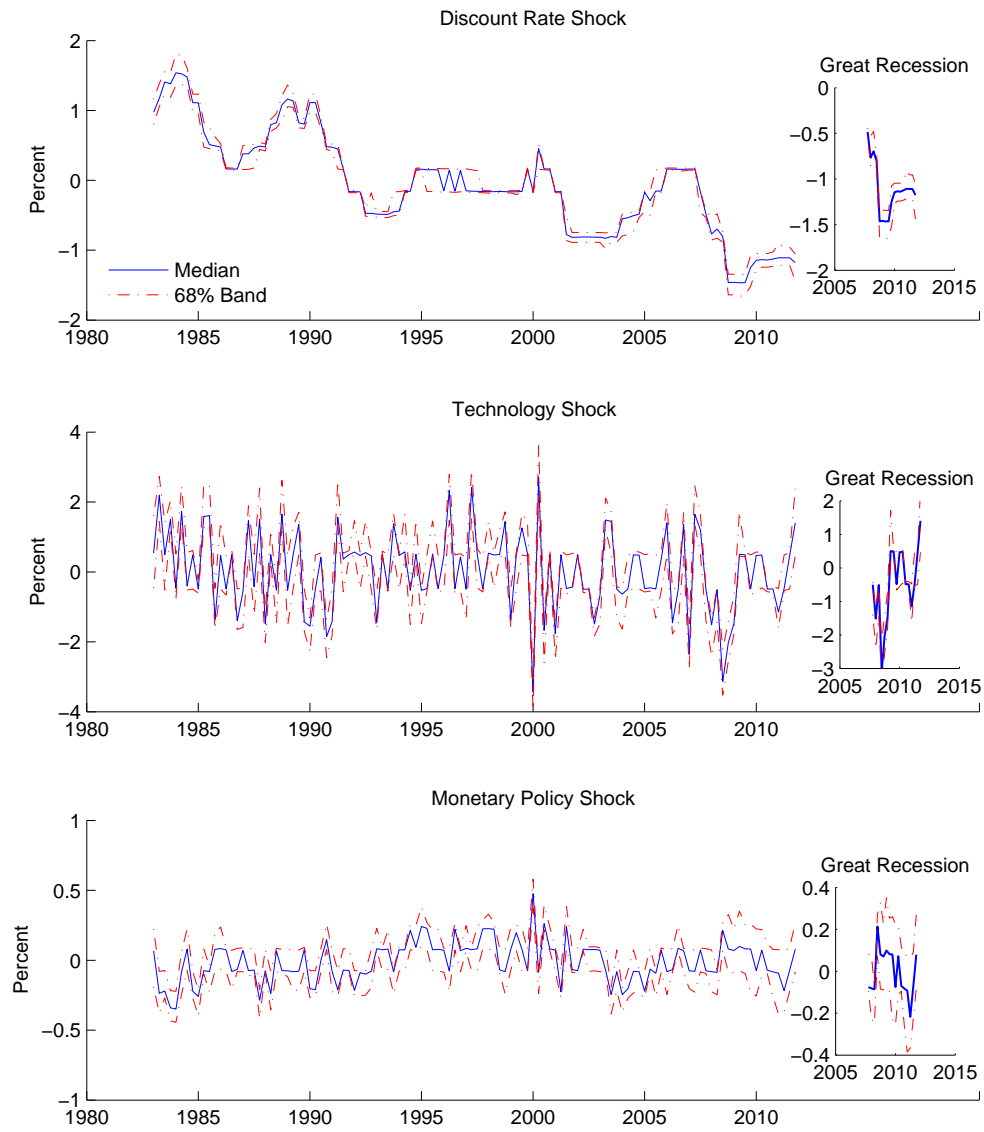
Note: The figure reports the difference between the median values of a shocked path, which introduces an unexpected increase in the discount rate at date 1 relative to the median values of the (unshocked) baseline path shown in Figure 2. The median responses were constructed by simulating 1,000,000 paths of the economy's variables.

Figure 4: The Effects of a Productivity Shock



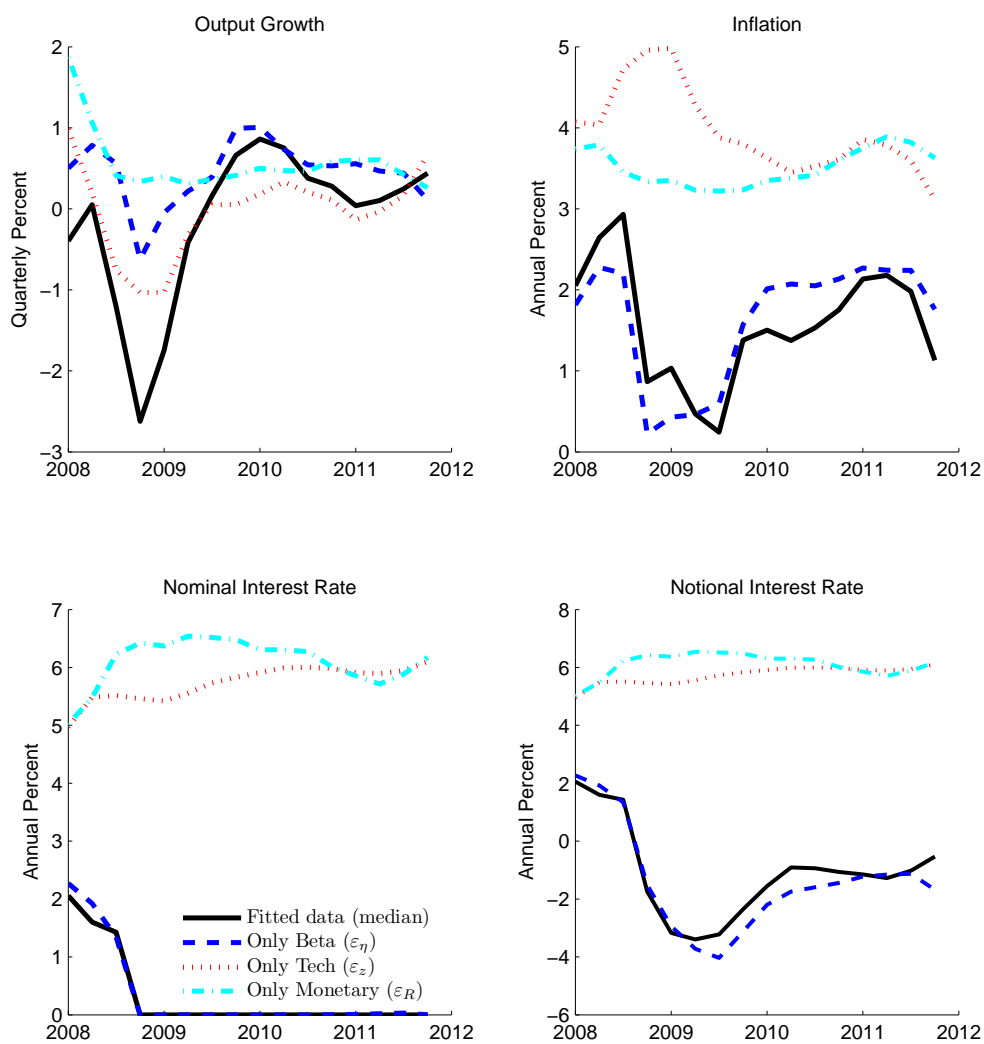
Note: The figure reports the difference between the median values of a shocked path, which introduces an unexpected increase in the level of productivity at date 1 relative to the median values of the (unshocked) baseline path shown in Figure 2. The median responses were constructed by simulating 1,000,000 paths of the economy's variables.

Figure 5: The Path of the Estimated Shocks



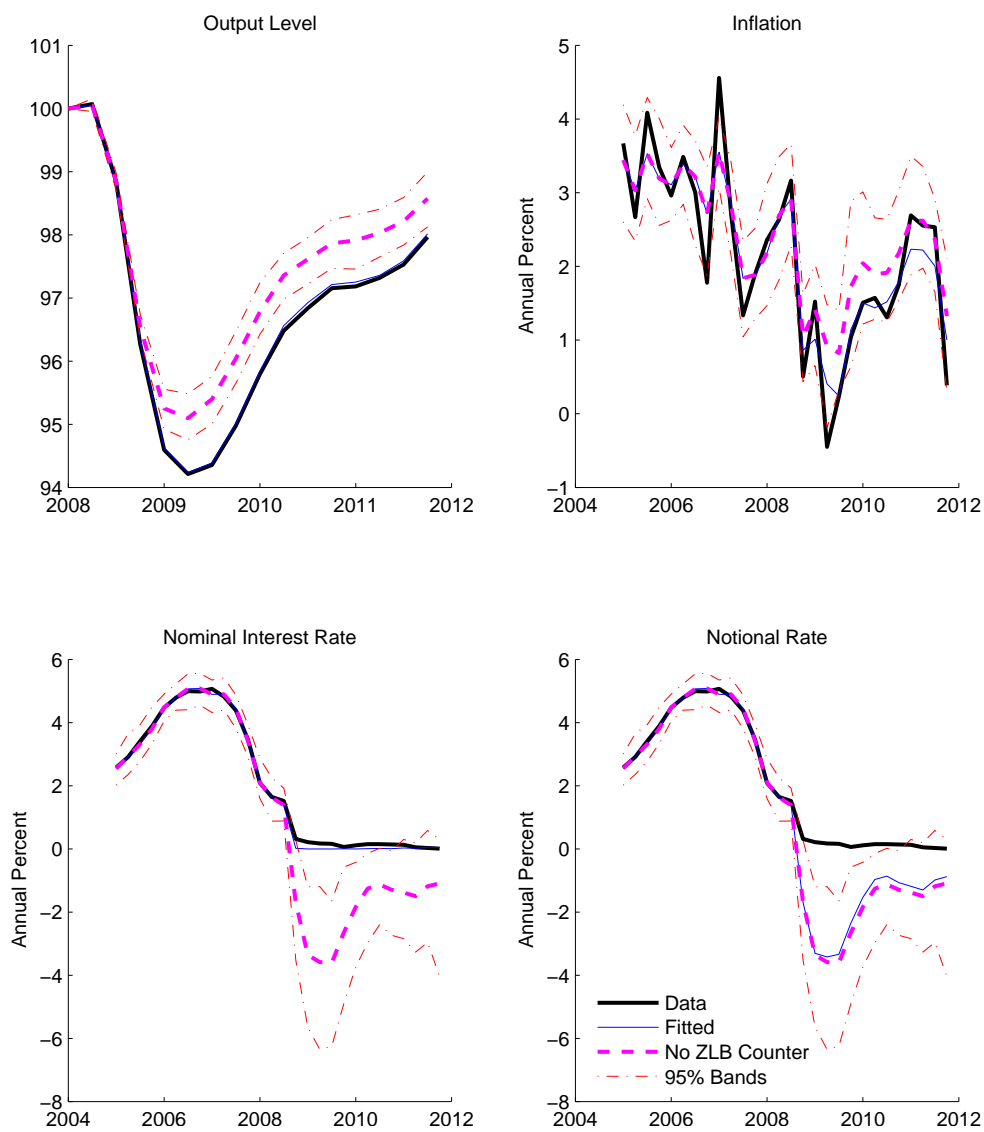
Note: For each draw $\vartheta \sim p(\vartheta | \mathbb{Y}_{1:T})$, we sample once from $p(\mathbb{S}_{1:T} | \mathbb{Y}_{1:T}, \vartheta)$ using the particle filter and report $f(\mathbb{S}_{1:T})$ for the appropriate function $f(\cdot)$. We draw 1000 times from our posterior distribution.

Figure 6: The Contribution of the Estimated Shocks to the Great Recession



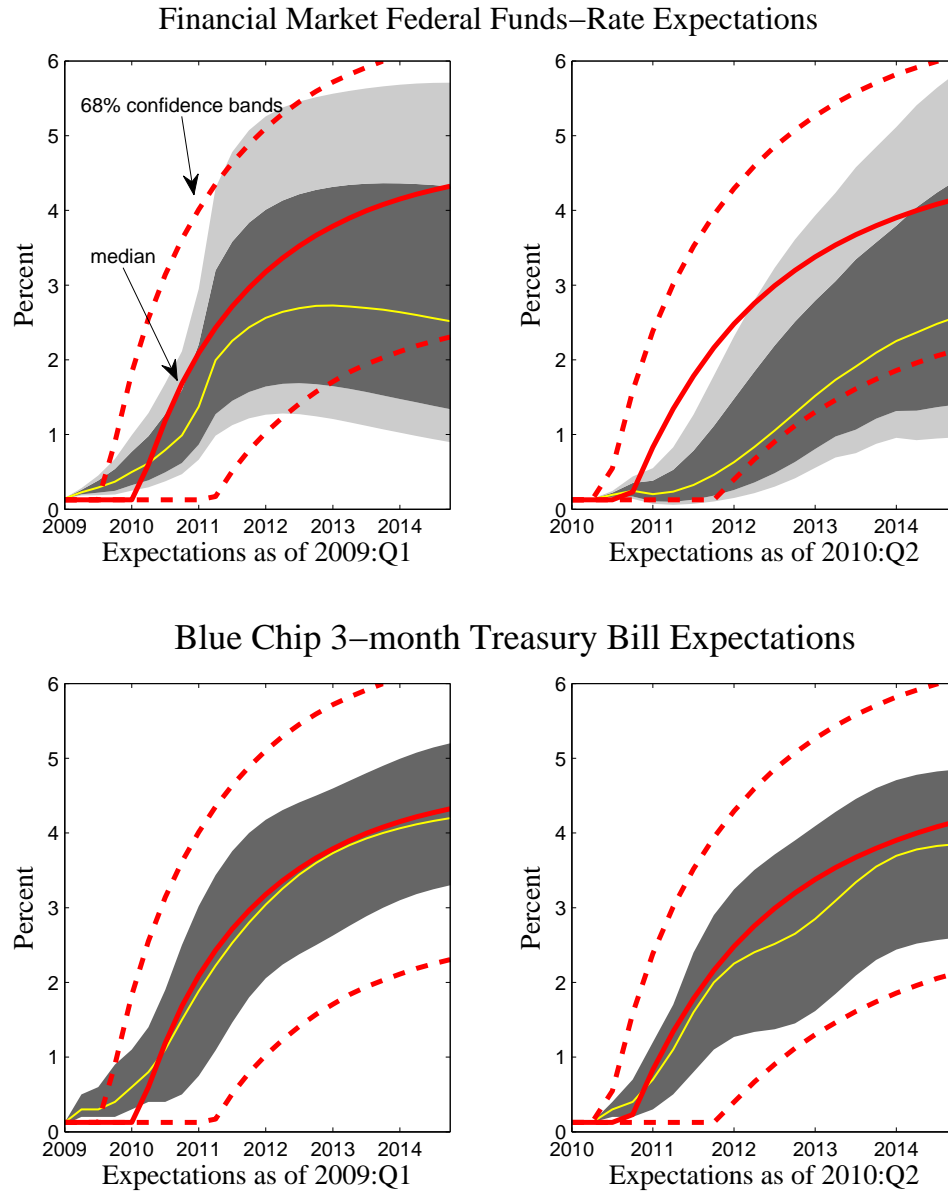
Note: We compute the counterfactual ‘Only Beta’ as follows. Starting in 2007:Q4, we take the estimated state (shown in Figure 1) as a starting value, and simulate the economy forward feeding in the smoothed $\varepsilon_{\eta,t}$ and assuming $\varepsilon_{Z,t} = \varepsilon_{R,t} = 0$. Analogous exercises are performed to plot the ‘Only Tech’ and ‘Only Monetary’ series.

Figure 7: The Contribution of the Lower Bound to the Great Recession



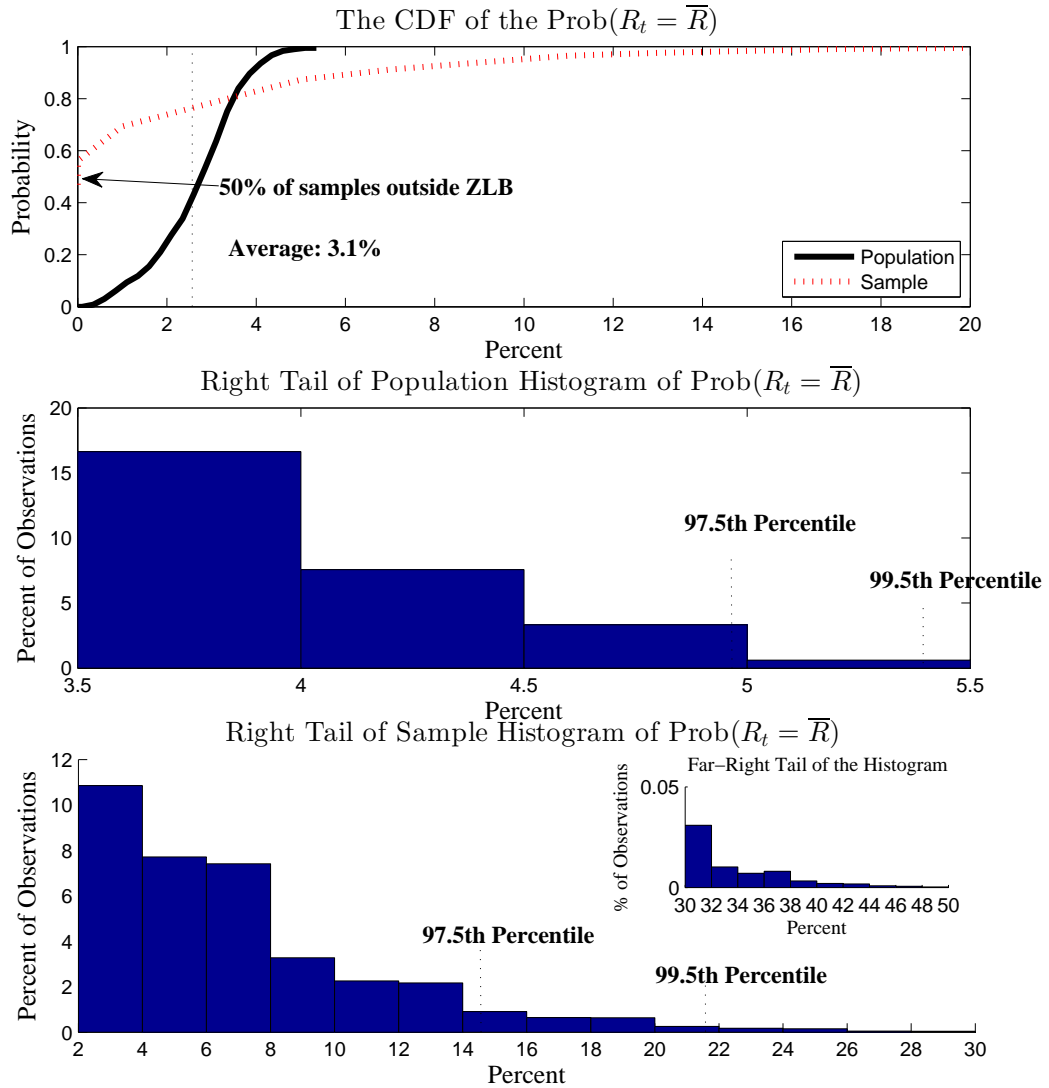
Note: We take the estimated value of the state (shown in figure 1) as a starting value, and simulate the economy forward feeding in the smoothed $(\varepsilon_{\eta,t}, \varepsilon_Z,t, \varepsilon_R,t)$ series but without imposing the lower bound.

Figure 8: The Expected Path of Nominal Interest Rates



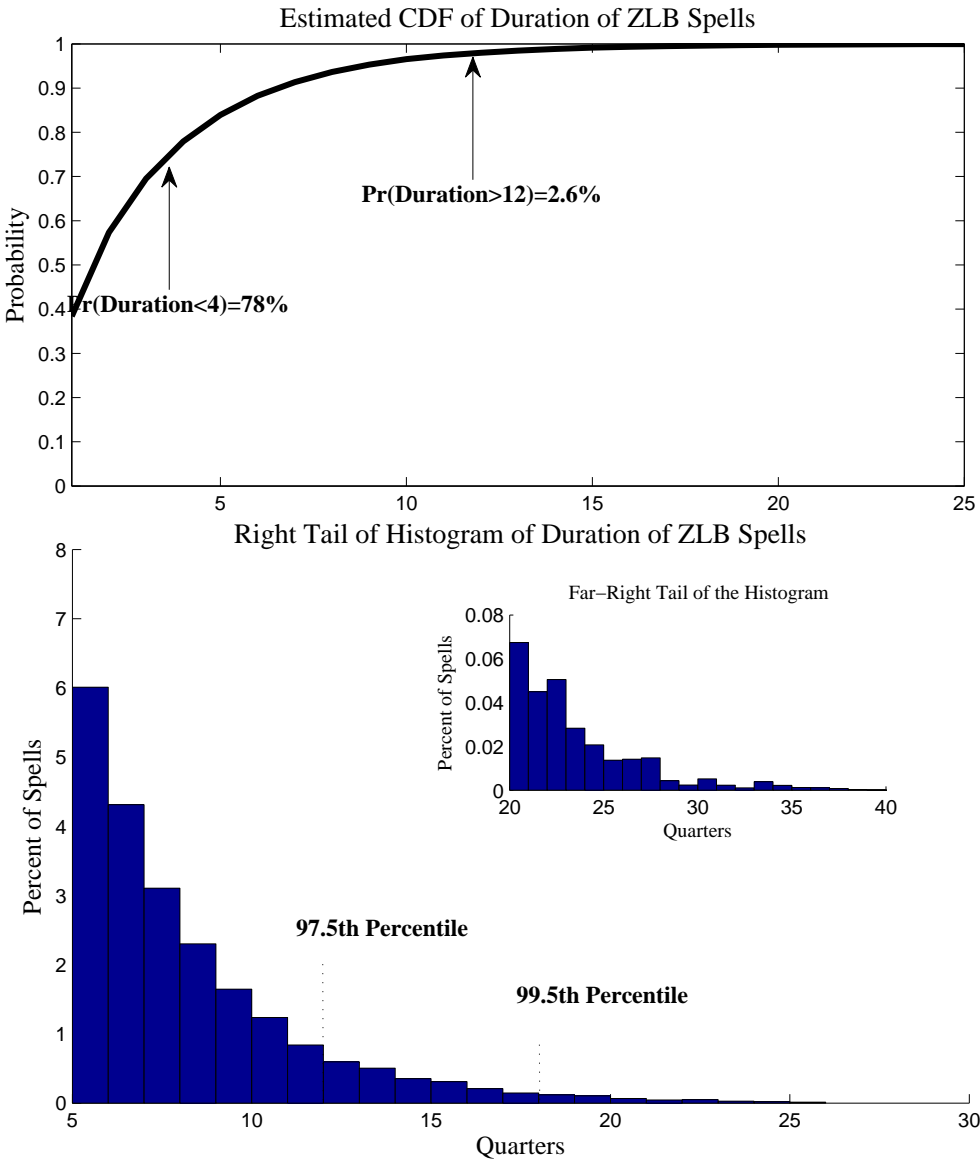
Note: Eurodollar quotes and implied three-month forward rates from swaps were used to estimate the median financial market federal funds-rate path from one quarter ahead to 40 quarters ahead. The dark and light shading represent the 70 and 90 percent confidence intervals respectively. Financial market quotes were taken from March 18, 2009 and June 16, 2010 to represent pre-FOMC market expectations for 2009:Q1 and 2010:Q2, respectively. The three month Treasury yield expectations are based on the Blue Chip Economic Indicators release from March 10, 2009 and June 10, 2010. Confidence bounds represent the mean of the 10 highest and lowest observations in the sample of 46 market participants surveyed in the Blue Chip release. The model paths for the nominal interest are computed using the posterior means of the parameter values, and the mean estimate of the state as initial conditions for 2009:Q1 and 2010:Q2. We then simulate 1,000,000 paths, each of length 24 quarters, and report the median value and 68th percentile in each quarter.

Figure 9: The Distribution of the Probability of Hitting the Lower Bound



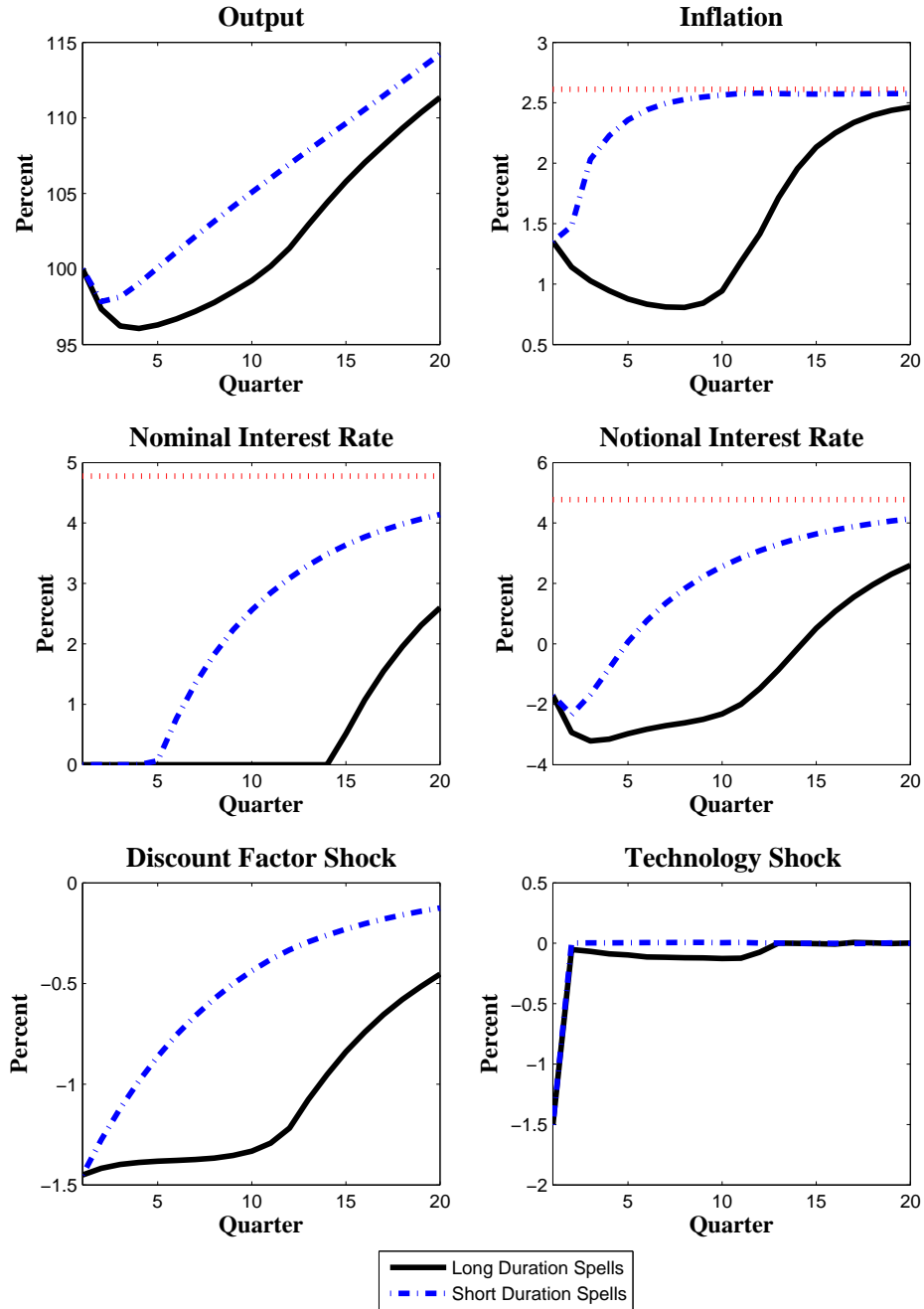
Note: For each draw $\vartheta \sim p(\vartheta | \mathbb{Y}_{1:T})$, we simulate the economy for 1,000,000 time periods and compute the fraction of time the economy is constrained by the ZLB to get the population estimate. To compute the small sample estimate, we break 1,000,000 time periods into bins of 116 time periods, compute the fraction of time that the economy is at the ZLB, and report that distribution (sample histogram). We draw 1000 times from our posterior distribution.

Figure 10: The Distribution of the Duration of a Lower Bound Spell



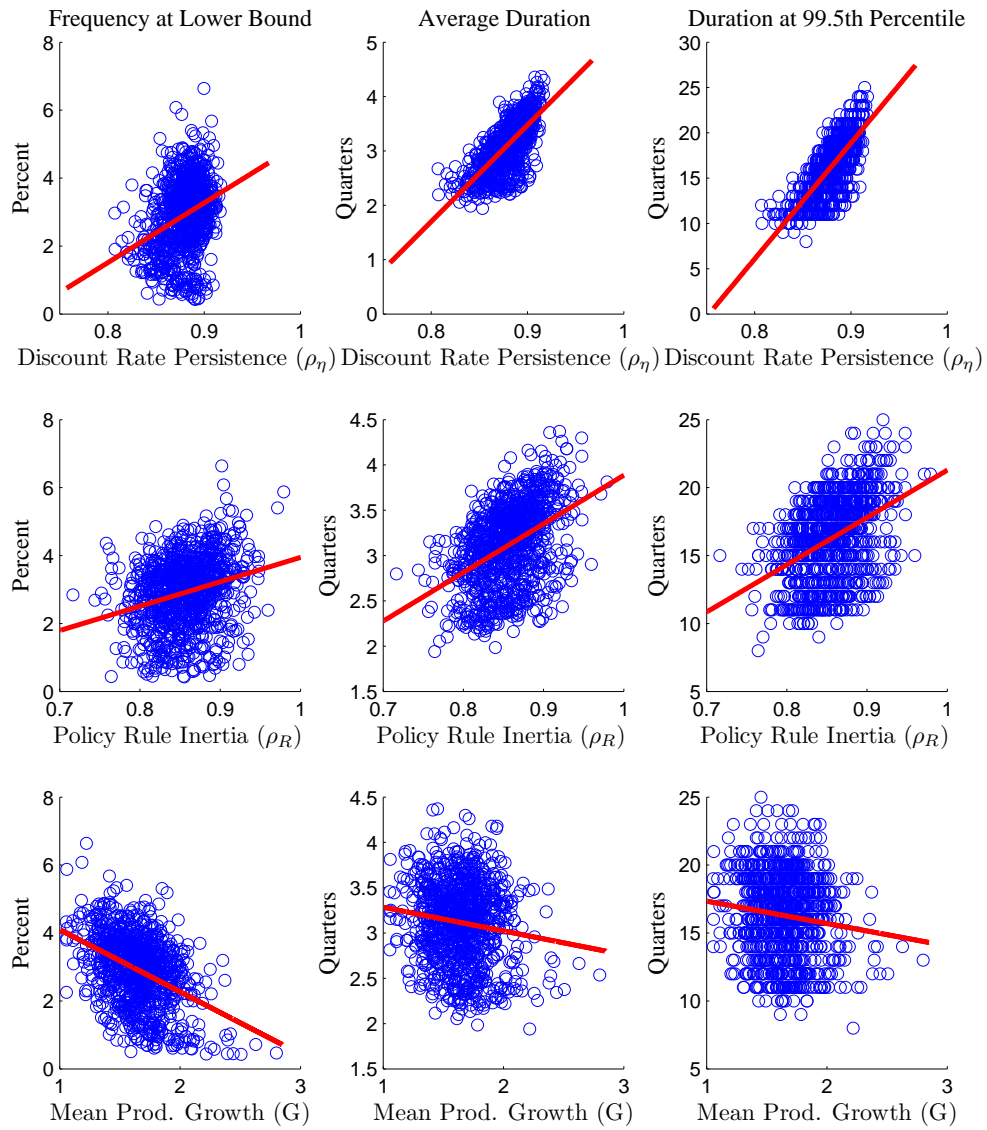
Note: For each draw $\vartheta \sim p(\vartheta|Y_{1:T})$, we simulate the economy for 1,000,000 time periods and compute the distribution of duration of ZLB episodes and report the CDF and right tail of the estimated distribution of spells. We draw 1000 times from our posterior distribution.

Figure 11: The Dynamics of Short and Long Lower Bound Spells



Note: The model responses are computed as follows. For both long and short duration spells, we use the posterior means of the parameter values, and the mean estimate of the state in 2008:Q4 as initial conditions. We then simulate 1,000,000 paths each with 20 quarterly observations. For each of those paths with these initial conditions, the economy is at the lower bound in period 1. The path for the long duration spells is constructed as the median value of spells which are at the lower bound for 12 consecutive quarters or longer. The median path for the short duration spell is constructed from the remaining simulated paths.

Figure 12: Scatter Plots of Frequency and Duration of Lower Bound Episodes



Note: For each draw $\vartheta \sim p(\vartheta | \mathbb{Y}_{1,T})$, we simulate the economy for 1,000,000 time periods and compute the distribution of duration of ZLB episodes and report the CDF and right tail of the estimated distribution of spells. We draw 1000 times from our posterior distribution.

Appendix

The appendix is divided in two sections. The first one characterizes the model's equilibrium in terms of time-invariant functions and uses that characterization to describe our solution algorithm. It also compares our solution algorithm with an algorithm that involves imposing the lower bound constraint in the context of the linearized equilibrium conditions. The second section discusses the evaluation of the likelihood function using the particle filter and the final section displays the linearized model equations.

A Characterizing and Solving the Model's Equilibrium

Before discussing our solution method, we discuss the model's equilibrium conditions. To do so, we write the model's decision rules and equilibrium conditions as time-invariant functions. Let $\mathbb{K} = h(\mathbb{K}_{-1}, \tau)$, where $\mathbb{K}_{-1} = (R_{-1}^*, \Pi_{-1}, \tilde{Y}_{-1})$ and $\tau = (\eta, \varepsilon_Z, \varepsilon_R)$. Also, h_π and h_y denote the second and third elements of the functions that comprise h . It is also convenient to define the residual functions:

$$\nu_c(\mathbb{K}_{-1}, \tau) = 0 \quad (\text{A.1})$$

$$\nu_\pi(\mathbb{K}_{-1}, \tau) = 0 \quad (\text{A.2})$$

where $\nu_c(\mathbb{K}_{-1}, \tau)$ and $\nu_\pi(\mathbb{K}_{-1}, \tau)$ are given by:

$$\begin{aligned} \nu_c(\mathbb{K}_{-1}, \tau) &= \frac{1}{W(\mathbb{K}_{-1}, \tau)} - \frac{\tilde{\beta} R(\mathbb{K}_{-1}, \tau)}{G\eta} \times E \left\{ \frac{\exp(-\varepsilon'_Z)}{W(\mathbb{K}, \tau') h_\pi(\mathbb{K}, \tau')} \mid \mathbb{K}_{-1}, \tau \right\} \\ \nu_\pi(\mathbb{K}_{-1}, \tau) &= \left(\frac{h_\pi(\mathbb{K}_{-1}, \tau)}{\bar{\Pi}} - 1 \right) \frac{h_\pi(\mathbb{K}_{-1}, \tau)}{\bar{\Pi}} \\ &\quad - \frac{\beta}{\eta} \times E \left\{ \frac{W(\mathbb{K}_{-1}, \tau)}{W(\mathbb{K}, \tau')} \left(\frac{h_\pi(\mathbb{K}, \tau')}{\bar{\Pi}} - 1 \right) \frac{h_\pi(\mathbb{K}, \tau')}{\bar{\Pi}} \frac{h_y(\mathbb{K}, \tau')}{h_y(\mathbb{K}_{-1}, \tau')} \mid \mathbb{K}_{-1}, \tau \right\} \\ &\quad + \frac{\epsilon - 1}{\varphi} - \frac{\epsilon}{\varphi} W(\mathbb{K}_{-1}, \tau) \end{aligned}$$

The functions, $W(\mathbb{K}_{-1}, \tau)$ and $A(\mathbb{K}_{-1}, \tau)$, are given by:

$$W(\mathbb{K}_{-1}, \tau) = A(\mathbb{K}_{-1}, \tau) h_y(\mathbb{K}_{-1}, \tau) - \tilde{\gamma} \left[1 - \frac{\varphi}{2} \left(\frac{\Pi_{-1}}{\bar{\Pi}} - 1 \right)^2 \right] \tilde{Y}_{-1} \exp(-\varepsilon_Z),$$

$$A(\mathbb{K}_{-1}, \tau) = 1 - \frac{\varphi}{2} \left(\frac{h_\pi(\mathbb{K}_{-1}, \tau)}{\bar{\Pi}} - 1 \right)^2.$$

In the above, the nominal interest rate is given by:

$$R(\mathbb{K}_{-1}, \tau) = \max[h_R(\mathbb{K}_{-1}, \tau), \bar{R}]$$

where $h_R(\mathbb{K}_{-1}, \tau)$ denotes the first element of h and is given by:

$$h_R(\mathbb{K}_{-1}, \tau) = \left(\frac{G\bar{\Pi}}{\beta} \right)^{1-\rho_R} (R_{-1}^*)^{\rho_R} \left(\frac{h_\pi(\mathbb{K}_{-1}, \tau)}{\bar{\Pi}} \right)^{\gamma_\pi} \left(\frac{h_y(\mathbb{K}_{-1}, \tau)}{\bar{Y}_{-1} \exp(-\varepsilon_Z)} \right)^{\gamma_y} \exp(\varepsilon_R).$$

For convenience, we have omitted two other important conditions regarding the model's equilibrium. These conditions reflect that we view our economy as the cashless limit of a model in which money enters the utility function. (See Eggertsson and Woodford (2003) for the functional form and further discussion of this issue.) These two conditions in the economy with money are a transversality condition involving household's cash holdings and a more fully specified monetary policy which requires the central bank to commit to increases in money growth in proportion to the central bank's inflation target in periods in which the interest rate is at its lower bound. These conditions rule out a second stationary equilibrium that is deflationary, because when monetary policy injects cash in this manner, the model's transversality condition is not satisfied. As the weight on cash balances in a household's utility function converges toward zero in this more fully specified version of the model, the economy's equilibrium conditions converge to the ones shown above.

A.1 An Equivalent Representation of the Model's Equilibrium

We do not approximate $h(\mathbb{K}_{t-1}, \tau_t)$ directly. Instead, following the ideas in Christiano and Fisher (2000), we approximate functions that are smoother and easier to approximate while still allowing for a closed-form mapping into $h(\mathbb{K}_{t-1}, \tau_t)$. To do so, we need to use an equivalent representation of the equilibrium conditions and rewrite the residual functions as:

$$\nu_c(\mathbb{K}_{-1}, \tau) = \nu_{c,1}(\mathbb{K}_{-1}, \tau) \mathbf{1}_{\{h_{R,1}(\mathbb{K}_{-1}, \tau) > \bar{R}\}} + \nu_{c,2}(\mathbb{K}_{-1}, \tau) \mathbf{1}_{\{h_{R,1}(\mathbb{K}_{-1}, \tau) \leq \bar{R}\}} \quad (\text{A.3})$$

$$\nu_\pi(\mathbb{K}_{-1}, \tau) = \nu_{\pi,1}(\mathbb{K}_{-1}, \tau) \mathbf{1}_{\{h_{R,1}(\mathbb{K}_{-1}, \tau) > \bar{R}\}} + \nu_{\pi,2}(\mathbb{K}_{-1}, \tau) \mathbf{1}_{\{h_{R,1}(\mathbb{K}_{-1}, \tau) \leq \bar{R}\}} \quad (\text{A.4})$$

where $\mathbf{1}_{\{D\}}$ is an indicator function which equals one if the condition D is true and zero otherwise. The functions $\nu_{c,1}(\cdot)$, $\nu_{c,2}(\cdot)$, $\nu_{\pi,1}(\cdot)$, $\nu_{\pi,2}(\cdot)$ are given by:

$$\begin{aligned} \nu_{c,1}(\mathbb{K}_{-1}, \tau) &= \frac{1}{W_1(\mathbb{K}_{-1}, \tau)} - \frac{\tilde{\beta} h_{R,1}(\mathbb{K}_{-1}, \tau)}{G\eta} \times E \left\{ \frac{\exp(-\varepsilon'_Z)}{W(\mathbb{K}, \tau') h_\pi(\mathbb{K}, \tau')} \mid \mathbb{K}_{-1}, \tau \right\} \\ \nu_{c,2}(\mathbb{K}_{-1}, \tau) &= \frac{1}{W_2(\mathbb{K}_{-1}, \tau)} - \frac{\tilde{\beta} \bar{R}}{G\eta} \times E \left\{ \frac{\exp(-\varepsilon'_Z)}{W(\mathbb{K}, \tau') h_\pi(\mathbb{K}, \tau')} \mid \mathbb{K}_{-1}, \tau \right\} \end{aligned}$$

and

$$\begin{aligned} \nu_{\pi,i}(\mathbb{K}_{-1}, \tau) &= \left(\frac{h_{\pi,i}(\mathbb{K}_{-1}, \tau)}{\bar{\Pi}} - 1 \right) \frac{h_{\pi,i}(\mathbb{K}_{-1}, \tau)}{\bar{\Pi}} \\ &\quad - \frac{\beta W_i(\mathbb{K}_{-1}, \tau)}{\eta} \times E \left\{ \frac{1}{W(\mathbb{K}, \tau')} \left(\frac{h_\pi(\mathbb{K}, \tau')}{\bar{\Pi}} - 1 \right) \frac{h_\pi(\mathbb{K}, \tau')}{\bar{\Pi}} \frac{h_y(\mathbb{K}, \tau')}{h_{y,i}(\mathbb{K}_{-1}, \tau')} \mid \mathbb{K}_{-1}, \tau \right\} \\ &\quad + \frac{\epsilon - 1}{\varphi} - \frac{\epsilon}{\varphi} W_i(\mathbb{K}_{-1}, \tau), \text{ for } i = 1, 2 \end{aligned}$$

where

$$W(\mathbb{K}_{-1}, \tau) = W_1(\mathbb{K}_{-1}, \tau) \mathbf{1}_{\{h_{R,1}(\mathbb{K}_{-1}, \tau) > \bar{R}\}} + W_2(\mathbb{K}_{-1}, \tau) \mathbf{1}_{\{h_{R,1}(\mathbb{K}_{-1}, \tau) \leq \bar{R}\}},$$

$$\begin{aligned}
A(\mathbb{K}_{-1}, \tau) &= A_1(\mathbb{K}_{-1}, \tau) \mathbf{1}_{\{h_{R,1}(\mathbb{K}_{-1}, \tau) > \bar{R}\}} + A_2(\mathbb{K}_{-1}, \tau) \mathbf{1}_{\{h_{R,1}(\mathbb{K}_{-1}, \tau) \leq \bar{R}\}}, \\
W_i(\mathbb{K}_{-1}, \tau) &= A_i(\mathbb{K}_{-1}, \tau) h_{y,i}(\mathbb{K}_{-1}, \tau) - \gamma \left[1 - \frac{\varphi}{2} \left(\frac{\bar{\Pi}_{-1}}{\bar{\Pi}} - 1 \right)^2 \right] \tilde{Y}_{-1} \exp(-\varepsilon_Z), \\
A_i(\mathbb{K}_{-1}, \tau) &= 1 - \frac{\varphi}{2} \left(\frac{h_{\pi,i}(\mathbb{K}_{-1}, \tau)}{\bar{\Pi}} - 1 \right)^2 \text{ for } i = 1, 2.
\end{aligned}$$

The decisions rules for inflation and output satisfy:

$$h_\pi(\mathbb{K}_{-1}, \tau) = h_{\pi,1}(\mathbb{K}_{-1}, \tau) \mathbf{1}_{\{h_{R,1}(\mathbb{K}_{-1}, \tau) > \bar{R}\}} + h_{\pi,2}(\mathbb{K}_{-1}, \tau) \mathbf{1}_{\{h_{R,1}(\mathbb{K}_{-1}, \tau) \leq \bar{R}\}} \quad (\text{A.5})$$

$$h_y(\mathbb{K}_{-1}, \tau) = h_{y,1}(\mathbb{K}_{-1}, \tau) \mathbf{1}_{\{h_{R,1}(\mathbb{K}_{-1}, \tau) > \bar{R}\}} + h_{y,2}(\mathbb{K}_{-1}, \tau) \mathbf{1}_{\{h_{R,1}(\mathbb{K}_{-1}, \tau) \leq \bar{R}\}}, \quad (\text{A.6})$$

while the notional rate when above the lower bound is given by:

$$h_{R,1}(\mathbb{K}_{-1}, \tau) = \left(\frac{G\bar{\Pi}}{\beta} \right)^{1-\rho_R} (R_{-1}^*)^{\rho_R} \left(\frac{h_{\pi,1}(\mathbb{K}_{-1}, \tau)}{\bar{\Pi}} \right)^{\gamma_\pi} \left(\frac{h_{y,1}(\mathbb{K}_{-1}, \tau)}{\tilde{Y}_{-1} \exp(-\varepsilon_Z)} \right)^{\gamma_y} \exp(\varepsilon_R). \quad (\text{A.7})$$

The index $i = 1, 2$, associates a function with the interest-rate regime in which the notional interest rate, R^* , is either above or below the lower bound. Because functions such $h_\pi(\mathbb{K}_{-1}, \tau)$ depend directly on the indicator function, we expect them to have a kink or non-differentiability. By contrast, the counterpart functions that are indexed by the the interest-rate regime, i , do not depend on the current indicator function and thus are more likely to be smooth.

The regime-specific functions still depend on a secondary effect that the kink has through its expectation in the next period. This secondary effect occurs through the expectation terms of $\nu_{\pi,i}$ and $\nu_{c,i}$ for $i = 1, 2$. For $\nu_{c,i}$, for example, the future value of the indicator function enters through $W(\mathbb{K}, \tau')$ or $h_\pi(\mathbb{K}, \tau')$ though the indicator function does not affect \mathbb{K} which is determined from the regime-specific functions. Following the arguments in Christiano and Fisher (2000), the secondary effects of the kink on the regime-specific functions should be small because of the presence of the expectations operator, which involves summing over the future states of τ . As we increase the number of discrete exogenous states, the regime-specific functions should become smoother. While our approach of using relatively smooth functions is similar to Christiano and Fisher (2000), we do not parameterize the expectations as in Christiano and Fisher (2000). The difference is that in our application there is no closed-form mapping between the two expectations in our residual functions and the model's decision rules. However, we are still able to focus on relatively smooth functions by approximating functions that do not depend on the current indicator of the interest-rate regime.

A.2 Solution Algorithm

To solve for these decision rules, we first approximate the AR(1) shock processes using discrete Markov chains. For each individual shock process, we follow Rouwenhorst (1995) to determine its support and transition matrix. Given this procedure, the vector $\tau \in [\tau_1, \tau_2, \dots, \tau_{N_\tau}]$ and has probability mass function $\Phi(\tau_l | \tau)$ for $l = 1, 2, \dots, N_\tau$. In estimating the model, we used 8 discrete values for technology and monetary innovations and 12 discrete values for the discount rate shock so that $N_\tau = 768$.

Using discrete Markov processes for the shocks, we approximate the functions:

$$\begin{aligned} V_i(\mathbb{K}_{-1}, \tau) &\approx \widehat{V}_i(\mathbb{K}_{-1}, \tau; a_{i,\tau}) = T(\varphi(\mathbb{K}_{-1})) a_{i,\tau} \\ W_i(\mathbb{K}_{-1}, \tau) &\approx \widehat{W}_i(\mathbb{K}_{-1}, \tau; b_{i,\tau}) = \exp\{T(\varphi(\mathbb{K}_{-1})) b_{i,\tau}\}, \end{aligned}$$

where $V_i(\mathbb{K}_{-1}, \tau)$ is defined as:

$$V_i(\mathbb{K}_{-1}, \tau) = \sum_{l=1}^{N_\tau} \left\{ \frac{1}{W(\mathbb{K}, \tau_l)} \left(\frac{h_\pi(\mathbb{K}, \tau_l)}{\bar{\Pi}} - 1 \right) \frac{h_\pi(\mathbb{K}, \tau_l)}{\bar{\Pi}} \frac{h_y(\mathbb{K}, \tau_l)}{h_{y,i}(\mathbb{K}_{-1}, \tau)} \right\} \Phi(\tau_l | \tau),$$

with $\mathbb{K} = h_i(\mathbb{K}_{-1}, \tau)$. Also, the vectors $a_{i,\tau}$ and $b_{i,\tau}$ are $N_{\mathbb{K}} \times 1$ vectors of parameters for $i = 1, 2$. The $1 \times N_{\mathbb{K}}$ vector $T(x)$ in Tensor notation takes the form:

$$T(x) = [T_1(x_1) \otimes T_2(x_2) \otimes T_3(x_3)]$$

where $T_j(x_j) = [T_{j,0}(x_j), \dots, T_{j,N_j-1}(x_j)]$ is a $1 \times N_j$ vector consisting of Chebyshev polynomials for $j = 1, 2, 3$. Accordingly, $T_{j,k_j-1}(x_j) : [-1, 1] \rightarrow [-1, 1]$ for $k_j = 1, \dots, N_j$. For each of our state variables, we use $\varphi_j : [\underline{\mathbb{K}}_j, \bar{\mathbb{K}}_j] \rightarrow [-1, 1]$ for $j = 1, 2, 3$, where $x_j = \varphi(\mathbb{K}_j) = \frac{2(\mathbb{K}_j - 1 - \underline{\mathbb{K}}_j)}{\bar{\mathbb{K}}_j - \underline{\mathbb{K}}_j}$ and x is the 1×3 vector, $x = [x_1, x_2, x_3]$. From these definitions, it follows that $N_{\mathbb{K}} = N_1 N_2 N_3$.

Our strategy involves finding a^* and b^* such that

$$\nu_{c,i}(\mathbb{K}_{-1,1,k_1}^*, \mathbb{K}_{-1,2,k_2}^*, \mathbb{K}_{-1,3,k_3}^*, \tau_l; a^*, b^*) = 0, \quad (\text{A.8})$$

$$\nu_{\pi,i}(\mathbb{K}_{-1,1,k_1}^*, \mathbb{K}_{-1,2,k_2}^*, \mathbb{K}_{-1,3,k_3}^*, \tau_l; a^*, b^*) = 0, \quad (\text{A.9})$$

for $i = 1, 2$, $l = 1, 2, \dots, N_\tau$, $k_j = 1, 2, \dots, N_j$, $j = 1, 2, 3$, and for $l = 1, 2, \dots, N_\tau$. In the above, the state variables, \mathbb{K}_{-1,j,k_j}^* , are evaluated at the roots of their respective Chebychev polynomials so that $\mathbb{K}_{-1,j,k_j}^* = \varphi^{-1}\left(x_{j,k_j}^*\right)$ where $x_{j,k_j}^* = \cos\left(\frac{\pi(k_j - 0.5)}{N_j}\right)$ for $k_j = 1, 2, \dots, N_j$ and $j = 1, 2, 3$. Also, a^* and b^* are the $1 \times 2N_\tau N_{\mathbb{K}}$ vectors of metaparameters that satisfy the system of equations defined by (A.8)-(A.9).

Before describing how we compute a^* and b^* , we show there is a closed-form mapping from $V_i(\mathbb{K}_{-1}, \tau)$ and $W_i(\mathbb{K}_{-1}, \tau)$ to the decision rules, $h(\mathbb{K}_{-1}, \tau)$. We describe this mapping using our approximation of these functions: $\widehat{V}_i(\mathbb{K}_{-1}, \tau; a_{i,\tau})$ and $\widehat{W}_i(\mathbb{K}_{-1}, \tau; b_{i,\tau})$. These approximated functions then map into $\widehat{h}(\mathbb{K}_{-1}, \tau; a, b)$, which determine the notional interest rate, inflation, and output.

This mapping works as follows. Given the functions $\widehat{V}_i(\mathbb{K}_{-1}, \tau; a_{i,\tau})$ and $\widehat{W}_i(\mathbb{K}_{-1}, \tau; b_{i,\tau})$, we can determine $\widehat{h}_{\pi,i}(\mathbb{K}_{-1}, \tau; a_{i,\tau}, b_{i,\tau})$ as the positive root of the following quadratic equation:

$$\left(\frac{\widehat{h}_{\pi,i}(\mathbb{K}_{-1}, \tau)}{\bar{\Pi}} - 1 \right) \frac{\widehat{h}_{\pi,i}(\mathbb{K}_{-1}, \tau)}{\bar{\Pi}} - \frac{\beta \widehat{W}_i(\mathbb{K}_{-1}, \tau; b_{i,\tau})}{\exp(\eta)} \widehat{V}_i(\mathbb{K}_{-1}, \tau; a_{i,\tau}) + \frac{\epsilon - 1}{\varphi} - \frac{\epsilon}{\varphi} \widehat{W}_i(\mathbb{K}_{-1}, \tau; b_{i,\tau}) = 0,$$

where for convenience we have suppressed that $\widehat{h}_{\pi,i}(\mathbb{K}_{-1}, \tau; a_{i,\tau}, b_{i,\tau})$ depends on the metaparameters, $a_{i,\tau}, b_{i,\tau}$. We use the positive root from this equation, because that root implies $\Pi > 0$, while the negative one implies $\Pi < 0$. (Since this is the gross inflation rate, the negative root corresponds to a non-positive price level given $P_{-1} > 0$.)

With regime-specific inflation determined in this manner, the approximation for the region-specific

decision rules for \tilde{Y} are given by:

$$\hat{h}_{y,i}(\mathbb{K}_{-1}, \tau; a_{i,\tau}, b_{i,\tau}) = \hat{A}_i(\mathbb{K}_{-1}, \tau; a_{i,\tau}, b_{i,\tau})^{-1} \left\{ \hat{W}_i(\mathbb{K}_{-1}, \tau; b_{i,\tau}) + \tilde{\gamma} \left[1 - \frac{\varphi}{2} \left(\frac{\Pi_{-1}}{\Pi} - 1 \right)^2 \right] \tilde{Y}_{-1} \exp(-\varepsilon_Z) \right\}$$

The notional rate in the first regime is given by applying $\hat{h}_{\pi,1}(\mathbb{K}_{-1}, \tau; a_{i,\tau}, b_{i,\tau})$ and $\hat{h}_{y,1}(\mathbb{K}_{-1}, \tau; a_{i,\tau}, b_{i,\tau})$ in equation (A.7). This allows us to obtain $\hat{h}(\mathbb{K}_{-1}, \tau; a_\tau, b_\tau)$ and $\hat{W}(\mathbb{K}_{-1}, \tau; a_\tau, b_\tau)$, where $a_\tau = (a'_{1,\tau}, a'_{2,\tau})$ and $b_\tau = (b'_{1,\tau}, b'_{2,\tau})$ are $1 \times 2N_{\mathbb{K}}$ vectors.

We use an iterative procedure to find a^* and b^* . Before starting these iterations, we compute:

$$\mathbb{T} = T_1 \otimes T_2 \otimes T_3$$

where \mathbb{T} is an $N_{\mathbb{K}} \times N_{\mathbb{K}}$ consisting of:

$$T_j = \begin{pmatrix} T_{j,0}(\varphi(\mathbb{K}_{-1,j,1}^*)) & \cdot & \cdot & \cdot & T_{j,N_j-1}(\varphi(\mathbb{K}_{-1,j,1}^*)) \\ \cdot & & & & \cdot \\ \cdot & & & & \cdot \\ T_{j,0}(\varphi(\mathbb{K}_{-1,j,N_j}^*)) & \cdot & \cdot & \cdot & T_{j,N_j-1}(\varphi(\mathbb{K}_{-1,j,N_j}^*)) \end{pmatrix},$$

for $j = 1, 2, 3$.

For the iterations, suppose that an initial vectors of parameters for a_τ and b_τ are available. Then using the mapping discussed above, we compute:

$$\hat{Z}_{V,i}(\mathbb{K}_{-1}, \tau; a, b) = \sum_{l=1}^{N_\tau} \frac{1}{\hat{W}(\hat{h}_i(\mathbb{K}_{-1}^*, \tau), \tau_l)} \left(\frac{\hat{h}_\pi(\hat{h}_i(\mathbb{K}_{-1}, \tau), \tau_l)}{\Pi} - 1 \right) \times \frac{\hat{h}_\pi(\hat{h}_i(\mathbb{K}_{-1}, \tau), \tau_l) \hat{h}_y(\hat{h}_i(\mathbb{K}_{-1}, \tau), \tau_l)}{\Pi \hat{h}_{y,i}(\mathbb{K}_{-1}, \tau)} \Phi(\tau_l | \tau)$$

$$\hat{Z}_{W,1}(\mathbb{K}_{-1}, \tau; a, b) = \log\left(\frac{G\eta}{\beta}\right) - \log(\hat{h}_{R,1}(\mathbb{K}_{-1}, \tau)) - \log \left[\sum_{l=1}^{N_\tau} \frac{\exp(-\varepsilon'_Z)}{\hat{W}(\hat{h}_i(\mathbb{K}_{-1}, \tau), \tau_l)} \frac{\Phi(\tau_l | \tau)}{\hat{h}_\pi(\hat{h}_i(\mathbb{K}_{-1}, \tau), \tau_l)} \right]$$

$$\hat{Z}_{W,2}(\mathbb{K}_{-1}, \tau; a, b) = \log\left(\frac{G\eta}{\beta R}\right) - \log \left[\sum_{l=1}^{N_\tau} \frac{\exp(-\varepsilon'_Z)}{\hat{W}(\hat{h}_i(\mathbb{K}_{-1}^*, \tau), \tau_l)} \frac{\Phi(\tau_l | \tau)}{\hat{h}_\pi(\hat{h}_i(\mathbb{K}_{-1}, \tau), \tau_l)} \right],$$

where we evaluate \mathbb{K}_{-1} at the $N_{\mathbb{K}}$ Chebychev roots given by $\mathbb{K}_{-1}^* = (\mathbb{K}_{-1,1,k_1}^*, \mathbb{K}_{-1,2,k_2}^*, \mathbb{K}_{-1,3,k_3}^*)$ where $k_j = 1, 2, \dots, N_j$ for $j = 1, 2, 3$. For a given vector τ_l , we find new vectors a_{i,τ_l}^n , b_{i,τ_l}^n using the rules:

$$a_{i,\tau_l}^n = \mathbb{T}^{-1} \hat{Z}_{V,i}(\mathbb{K}_{-1}^*, \tau_l; a, b)$$

$$b_{i,\tau_l}^n = \mathbb{T}^{-1} \hat{Z}_{W,i}(\mathbb{K}_{-1}^*, \tau_l; a, b),$$

for $i = 1, 2$ and where $\hat{Z}_{V,i}(\mathbb{K}_{-1}^*, \tau_l; a, b)$ and $\hat{Z}_{W,i}(\mathbb{K}_{-1}^*, \tau_l; a, b)$ are $N_{\mathbb{K}} \times 1$ vectors constructed by evaluating these functions at the $N_{\mathbb{K}}$ Chebychev roots and stacking them appropriately. We update these parameters for $i = 1, 2$ and $l = 1, 2, \dots, N_\tau$ and iterate until a and b converge. Note that there

can be substantial gains from parallelizing the update step, because this step is independent across the different values of τ_l , helping make this algorithm computationally efficient. Moreover, by deriving a closed form solution for updating the metaparameters, we avoid the use of a computationally-intensive Newton-Raphson algorithm.

In estimating the model, we set each univariate basis of the Chebychev polynomials to two so that $a_{i,\tau}$ and $b_{i,\tau}$ each consist of 8 parameters for $i = 1, 2$. Thus, the the law of motion for the endogenous state, $\mathbb{K} = \widehat{h}(\mathbb{K}_{-1}, \tau; a_\tau, b_\tau)$ is characterized by 32 parameters for a given value of τ . With $N_\tau = 768$, a and b each consist of 12,228 parameters and there are 24,576 total parameters characterizing the policy functions for output, inflation, and the notional interest rate.

We find that there are two different a^* and b^* that satisfy the system of equations, (A.8)-(A.9). One solution corresponds to outcomes in which the unconditional average rate of inflation is positive and the other to outcomes in which the unconditional average of inflation is negative. To focus on the former, we use the nonstochastic steady state associated with the central bank's target for inflation to construct the starting guess for a^* and b^* . We find that in practice this starting guess never converges to the solution in which the unconditional average inflation rate is negative. In addition, using this starting guess, we verified *ex post* that each of the 1000 draws from the posterior distribution of the parameters implied an average inflation rate well above zero.

A.3 Comparing Solution Algorithms

We compare our solution algorithm to the one described in Erceg and Lindé (2012) and Bodenstein, Guerrieri, and Gust (2012). This algorithm involves log-linearizing the equilibrium conditions around the non-stochastic steady state to obtain:

$$\begin{aligned}\widehat{\lambda}_t &= \widehat{r}_t - \log \eta_t + E_t \left\{ \widehat{\lambda}_{t+1} - \widehat{\pi}_{t+1} - \varepsilon_{Z,t+1} \right\} \\ (1 - \widetilde{\gamma})\widehat{\lambda}_t &= -\widehat{y}_t + \widetilde{\gamma}\widehat{y}_{t-1} - \widetilde{\gamma}\varepsilon_{Z,t} \\ (1 - \widetilde{\gamma})\widehat{\omega}_t &= \widehat{y}_t - \widetilde{\gamma}\widehat{y}_{t-1} + \widetilde{\gamma}\varepsilon_{Z,t} \\ \widehat{\pi}_t &= \beta E_t \widehat{\pi}_{t+1} + \frac{\epsilon - 1}{\varphi} \widehat{\omega}_t,\end{aligned}$$

where the lower case refers to the log of a variable and a hat denotes the deviation of a variable from its value in nonstochastic steady state and $\widetilde{\gamma} = \frac{\gamma}{G}$. This system of equations can be reduced to the following two equations for output and inflation:

$$\begin{aligned}\widehat{y}_t &= \frac{\widetilde{\gamma}}{1 + \widetilde{\gamma}} \widehat{y}_{t-1} + \frac{1}{1 + \widetilde{\gamma}} E_t \widehat{y}_{t+1} + \frac{1 - \widetilde{\gamma}}{1 + \widetilde{\gamma}} \log \eta_t - \frac{\widetilde{\gamma}}{1 + \widetilde{\gamma}} \varepsilon_{Z,t} - \frac{1 - \widetilde{\gamma}}{1 + \widetilde{\gamma}} E_t \left\{ \widehat{r}_t - \widehat{\pi}_{t+1} - \frac{1}{1 - \widetilde{\gamma}} \varepsilon_{Z,t+1} \right\} \\ \widehat{\pi}_t &= \beta E_t \widehat{\pi}_{t+1} + \frac{\epsilon - 1}{\varphi} \frac{1}{1 - \widetilde{\gamma}} \{ \widehat{y}_t - \widetilde{\gamma}\widehat{y}_{t-1} + \widetilde{\gamma}\varepsilon_{Z,t} \}.\end{aligned}$$

The monetary policy rule can be written as:

$$\begin{aligned}\widehat{r}_t &= \max[\bar{r} - r_{ss}, \widehat{r}_t^*] \\ \widehat{r}_t^* &= \rho_R \widehat{r}_{t-1}^* + \gamma_\pi \widehat{\pi}_t + \gamma_y (\widehat{y}_t - \widehat{y}_{t-1} + \varepsilon_{Z,t}) + \varepsilon_{R,t},\end{aligned}$$

where r_{ss} denotes the nonstochastic steady state value of the log of the nominal interest rate. The above four equations jointly determine the behavior of output, inflation, the nominal interest rate, and the desired or notional interest rate.

The algorithm for solving this system of equations replaces the equation with the *max* operator with $\hat{r}_t = \hat{r}_t^* + m_t$, where m_t can be interpreted as an anticipated monetary policy shock. The sequence of current and future innovations to m_t are chosen so that if the notional rate falls below zero, the nominal interest rate is at the lower bound; otherwise, the nominal rate must equal the notional rate. With the innovations chosen in this way, the duration that the economy is at the lower bound is endogenous. For estimation purposes, this method is attractive, since it is easy to compute. However, we find that this algorithm can generate sizeable large differences from our projection method with relatively large Euler errors.

To demonstrate this finding, Figure B.1 compares the evolution of the economy from the estimated initial state in 2009:Q2 for the two different solution methods. For the projection method, the responses are identical to those shown in Figure 2. For these initial conditions, the median paths for output growth and inflation using the constrained-linear solution method lie substantially below those given by the projection method. Accordingly, the median path for the desired or notional rate is much lower, falling below -10 percent at its nadir, so that the duration of the lower bound spell is 14 quarters, compared to 5 quarters using the projection method. Figure B.1 shows the median path of the absolute value of the Euler errors, $\nu_c(\mathbb{K}_{-1}, \tau)$ and $\nu_\pi(\mathbb{K}_{-1}, \tau)$, that emerge from these two algorithms. The Euler errors at each date of the simulation are orders of magnitude larger for the constrained-linear method, suggesting that this algorithm is not accurate enough to provide a quantitative assessment of the lower bound constraint in the context of our model.

Figure B.2 compares the two solution algorithms for the 2006:Q1 initial conditions. In this case, the two solution algorithms yield similar results, suggesting that the constrained-linear solution may be appropriate for small shocks. However, for relatively large shocks or deviations from initial conditions, the application of this algorithm in our context becomes questionable.

B Likelihood Evaluation

After solving for the state transition equation,

$$\mathbb{S}_t = g_\vartheta(\mathbb{S}_{t-1}, \tau_t)$$

we need to map the variables computed in our model to observables. Let $\mathbb{Y}_t = (\Delta y_t, \pi_t, r_t)'$, denote the observed log GDP growth, log inflation and the log interest rate at time t , and let \tilde{Y}_t , Π_t , and R_t denote detrended output, level inflation and gross interest rate at time t computed in our model (these are just specific entries of the mapping $g_\vartheta(\mathbb{S}_{t-1}, \epsilon_t)$). The function $f_\vartheta(\mathbb{S}_t, \nu_t)$, is given by,

$$f_\vartheta(\mathbb{S}_t, \nu_t) = \begin{bmatrix} \log(\tilde{Y}_t) - \log(\tilde{Y}_{t-1}) + \log(G) + \varepsilon_{Z,t} + \sigma_{\Delta y_t} \nu_{1,t} \\ \log(\Pi_t) + \sigma_\pi \nu_{2,t} \\ \log(R_t) + \sigma_r \nu_{3,t} \end{bmatrix} \quad (\text{B.1})$$

Where $\nu_t \sim N(0, I_{3 \times 3})$. Such a nonlinear state space model does not permit a closed form solution to the likelihood function $p(\mathbb{Y}_{1:T}|\vartheta)$. A particle filter is one method of approximating such a likelihood

function. The algorithm is described in the box below.

Algorithm 2 A Particle Filter

```

given some  $\vartheta$ 
for  $i = 1, \dots, N$  do
    simulate  $\mathbb{S}_0^i \sim p_\vartheta(\cdot)$ 
    set  $W_t^i = \frac{1}{N}$ 
end for
for  $t = 1, \dots, T$  do
    for  $i = 1, \dots, N$  do
        simulate  $\tau_t^i \sim p_\vartheta(\tau_{t-1}^i, \cdot)$ 
        set  $\mathbb{S}_t^i = g_\vartheta(\mathbb{S}_t^i, \tau_t^i)$ , and  $\mathbb{S}_{1:t}^i = (\mathbb{S}_{1:t-1}^i, \mathbb{S}_t^i)$ 
        compute  $W_t^i = p_\vartheta(\mathbb{Y}_t | \mathbb{S}_t^i) W_{t-1}^i$ 
    end for
    for  $i = 1, \dots, N$  do
        normalize the weight,  $w_t^i = W_t^i / \sum_{i=1}^N W_t^i$ 
    end for
    compute likelihood contribution  $L_t = \sum W_t^i$ 
    resample  $N$  times with replacement from  $\{\mathbb{S}_{1:t}^i\}_{i=1}^N$ , where  $\mathbb{S}_{1:t}^i$  is drawn with probability  $w_t^i$ 
    for  $i = 1, \dots, N$  do
        set  $W_t^i = \frac{1}{N}$ 
    end for
end for
compute  $\hat{p}(\mathbb{Y}_{1:T} | \vartheta) = \prod_{t=1}^T L_t$ 

```

Note that drawing $\mathbb{S}_0 \sim p_\vartheta(\cdot)$ involves simulating from the ergodic distribution of states, drawing from $p_\vartheta(\tau_{t-1}, \cdot)$ is just simulating from (given our solution algorithm) discretized exogenous variables, and $p_\vartheta(\mathbb{Y}_t | \mathbb{S}_t)$ is the density of a normal distribution. We use systematic resampling to perform the resampling at each time period.

For computational reasons, we only store the most recent vector \mathbb{S}_t in memory. The algorithm was coded in Fortran and parallelized using MPI. After estimating our model using the surrogate algorithm described in the main text, our fitted values are obtained by re-running the particle filter at selected ϑ and drawing from $p(\mathbb{S}_{1:T} | \mathbb{Y}_{1:T}, \vartheta)$, then selecting the appropriate elements of $\mathbb{S}_{1:T}$.

B.1 Theoretical details of PMMH with Surrogate Transitions

Below we will sketch the proof that our algorithm has $p(\vartheta | \mathbb{Y}_{1:T})$ as its invariant distribution. At its heart, it is a Metropolis-Hastings algorithm on an extended space to include the vector of random variables that are used to evaluate the particle filter and uses as a proposal distribution, the transition kernel of a surrogate Markov chain. The surrogate Markov chain is constructed using the Metropolis-Hastings algorithm targeting the easy-to-compute distribution. More details are contained in Smith (2011).

We will use a joint distribution of parameters ϑ and vector of random variables u that are used to evaluate the particle filter as a target density of the Metropolis-Hastings algorithm. The approximation of the likelihood evaluated using the particle filter is then $\hat{p}(\mathbb{Y}_{1:T} | \vartheta) = p(\mathbb{Y}_{1:T} | \vartheta, u)$. Accordingly, our

target density is $p(\vartheta, u|\mathbb{Y}_{1:T}) \propto p(\mathbb{Y}_{1:T}|\vartheta, u)p(u|\vartheta)p(\vartheta)$ that has $p(\vartheta|\mathbb{Y}_{1:T})$, the posterior distribution of parameters given the data, as its marginal density. Here, $p(u|\vartheta)$ is the density of the vector of random variables u that are used to evaluate the particle filter given our vector of structural parameters ϑ .

Define the surrogate target density as $\tilde{p}(\vartheta, u|\mathbb{Y}_{1:T}) \propto \tilde{p}(\mathbb{Y}_{1:T}|\vartheta, u)p(u|\vartheta)\tilde{p}(\vartheta)$, where $\tilde{p}(\mathbb{Y}_{1:T}|\vartheta, u)$ is an approximation to the likelihood function (our easy-to-compute surrogate) and $\tilde{p}(\vartheta)$ is surrogate prior density of our parameters ϑ , not necessarily equal to the prior. We will use an approximate likelihood function does not depend on the vector u , so that $\tilde{p}(\mathbb{Y}_{1:T}|\vartheta, u) = \tilde{p}(\mathbb{Y}_{1:T}|\vartheta)$.

First we will construct a surrogate Markov chain using the Metropolis-Hastings algorithm using a proposal distribution $\tilde{Q}(\{\vartheta, u\}, \cdot)$ and target $\tilde{p}(\vartheta, u|\mathbb{Y}_{1:T})$. Second, we will use the resulting transition kernel as a proposal distribution in a Metropolis-Hastings algorithm targeting $p(\vartheta, u|\mathbb{Y}_{1:T})$. The proposal density for the surrogate transition step is, $\tilde{q}(\{\vartheta, u\}, \{\vartheta', u'\}) = \tilde{q}(\vartheta, \vartheta')p(u'|\vartheta')$. The acceptance probability of a Markov chain constructed using the Metropolis-Hastings algorithm using a proposal distribution $\tilde{Q}(\{\vartheta, u\}, \cdot)$ and target $\tilde{p}(\vartheta, u|\mathbb{Y}_{1:T})$ is,

$$\begin{aligned} \alpha_1(\{\vartheta, u\}, \{\vartheta', u'\}) &= \min \left\{ 1, \frac{\tilde{p}(\vartheta', u'|\mathbb{Y}_{1:T})\tilde{q}(\{\vartheta', u'\}, \{\vartheta, u\})}{\tilde{p}(\vartheta, u|\mathbb{Y}_{1:T})\tilde{q}(\{\vartheta, u\}, \{\vartheta', u'\})} \right\} \\ &= \min \left\{ 1, \frac{\tilde{p}(\mathbb{Y}_{1:T}|\vartheta', u')p(u'|\vartheta')\tilde{p}(\vartheta')\tilde{q}(\{\vartheta', u'\}, \{\vartheta, u\})}{\tilde{p}(\mathbb{Y}_{1:T}|\vartheta, u)p(u|\vartheta)\tilde{p}(\vartheta)\tilde{q}(\{\vartheta, u\}, \{\vartheta', u'\})} \right\} \\ &= \min \left\{ 1, \frac{\tilde{p}(\mathbb{Y}_{1:T}|\vartheta', u')p(u'|\vartheta')\tilde{p}(\vartheta')\tilde{q}(\vartheta', \vartheta)p(u|\vartheta)}{\tilde{p}(\mathbb{Y}_{1:T}|\vartheta, u)p(u|\vartheta)\tilde{p}(\vartheta)\tilde{q}(\vartheta, \vartheta')p(u'|\vartheta')} \right\} \\ &= \min \left\{ 1, \frac{\tilde{p}(\mathbb{Y}_{1:T}|\vartheta', u')\tilde{p}(\vartheta')\tilde{q}(\vartheta', \vartheta)}{\tilde{p}(\mathbb{Y}_{1:T}|\vartheta, u)\tilde{p}(\vartheta)\tilde{q}(\vartheta, \vartheta')} \right\} \\ &= \min \left\{ 1, \frac{\tilde{p}(\mathbb{Y}_{1:T}|\vartheta')\tilde{p}(\vartheta')\tilde{q}(\vartheta', \vartheta)}{\tilde{p}(\mathbb{Y}_{1:T}|\vartheta)\tilde{p}(\vartheta)\tilde{q}(\vartheta, \vartheta')} \right\} \\ &= \alpha_1(\vartheta, \vartheta'). \end{aligned}$$

By having our target and proposal density including $p(u|\vartheta)$, and our approximation of the marginal likelihood a deterministic function of ϑ , we can accept or reject the pair (ϑ, u) without reference to u , giving us our first stage acceptance probability given in the main body of the paper.

The transition kernel of the surrogate Markov chain constructed using this Metropolis-Hastings update with $\tilde{p}(\vartheta, u|\mathbb{Y}_{1:T})$ as a target density and proposal distribution $\tilde{Q}(\{\vartheta, u\}, \cdot)$ will be denoted as $S(\{\vartheta, u\}, \cdot)$, that by construction, satisfies detailed balance with $\tilde{p}(\vartheta, u|\mathbb{Y}_{1:T})$. That is,

$$\tilde{p}(\vartheta, u|\mathbb{Y}_{1:T})S(\{\vartheta, u\}, \{\vartheta', u'\}) = S(\{\vartheta', u'\}, \{\vartheta, u\})\tilde{p}(\vartheta', u'|\mathbb{Y}_{1:T})$$

or re-written,

$$\frac{\tilde{p}(\mathbb{Y}_{1:T}|\vartheta, u)p(u|\vartheta)\tilde{p}(\vartheta)}{\tilde{p}(\mathbb{Y}_{1:T}|\vartheta', u')p(u'|\vartheta')\tilde{p}(\vartheta')} = \frac{S(\{\vartheta', u'\}, \{\vartheta, u\})}{S(\{\vartheta, u\}, \{\vartheta', u'\})}.$$

If we define as a proposal distribution in a standard Metropolis-Hastings algorithm targeting $p(\vartheta, u|\mathbb{Y}_{1:T})$,

$Q(\{\vartheta, u\}, \cdot) = S(\{\vartheta, u\}, \cdot)$, we have an acceptance probability for $\vartheta' \neq \vartheta$ of,

$$\begin{aligned}
\alpha_2(\{\vartheta, u\}, \{\vartheta', u'\}) &= \min \left\{ 1, \frac{p(\vartheta', u' | \mathbb{Y}_{1:T}) q(\{\vartheta', u'\}, \{\vartheta, u\})}{p(\vartheta, u | \mathbb{Y}_{1:T}) q(\{\vartheta, u\}, \{\vartheta', u'\})} \right\} \\
&= \min \left\{ 1, \frac{p(\vartheta', u' | \mathbb{Y}_{1:T}) S(\{\vartheta', u'\}, \{\vartheta, u\})}{p(\vartheta, u | \mathbb{Y}_{1:T}) S(\{\vartheta, u\}, \{\vartheta', u'\})} \right\} \\
&= \min \left\{ 1, \frac{p(\mathbb{Y}_{1:T} | \vartheta', u') p(u' | \vartheta') p(\vartheta') S(\{\vartheta', u'\}, \{\vartheta, u\})}{p(\mathbb{Y}_{1:T} | \vartheta, u) p(u | \vartheta) p(\vartheta) S(\{\vartheta, u\}, \{\vartheta', u'\})} \right\} \\
&= \min \left\{ 1, \frac{p(\mathbb{Y}_{1:T} | \vartheta', u') p(u' | \vartheta') p(\vartheta') \tilde{p}(\mathbb{Y}_{1:T} | \vartheta, u) p(u | \vartheta) \tilde{p}(\vartheta)}{p(\mathbb{Y}_{1:T} | \vartheta, u) p(u | \vartheta) p(\vartheta) \tilde{p}(\mathbb{Y}_{1:T} | \vartheta', u') p(u' | \vartheta') \tilde{p}(\vartheta')} \right\} \\
&= \min \left\{ 1, \frac{p(\mathbb{Y}_{1:T} | \vartheta', u') p(\vartheta') \tilde{p}(\mathbb{Y}_{1:T} | \vartheta, u) \tilde{p}(\vartheta)}{p(\mathbb{Y}_{1:T} | \vartheta, u) p(\vartheta) \tilde{p}(\mathbb{Y}_{1:T} | \vartheta', u') \tilde{p}(\vartheta')} \right\} \\
&= \min \left\{ 1, \frac{\tilde{p}(\mathbb{Y}_{1:T} | \vartheta') p(\vartheta') \tilde{p}(\mathbb{Y}_{1:T} | \vartheta) \tilde{p}(\vartheta)}{\tilde{p}(\mathbb{Y}_{1:T} | \vartheta) p(\vartheta) \tilde{p}(\mathbb{Y}_{1:T} | \vartheta') \tilde{p}(\vartheta')} \right\} \\
&= \alpha_2(\vartheta, \vartheta').
\end{aligned}$$

Hence our PMMH with Surrogate Transitions algorithm is a particular implementation of the Metropolis-Hastings algorithm, so that $p(\vartheta, u | \mathbb{Y}_{1:T})$ is its invariant distribution by construction and $p(\vartheta | \mathbb{Y}_{1:T})$ is its marginal density.

B.2 Construction of the Surrogate

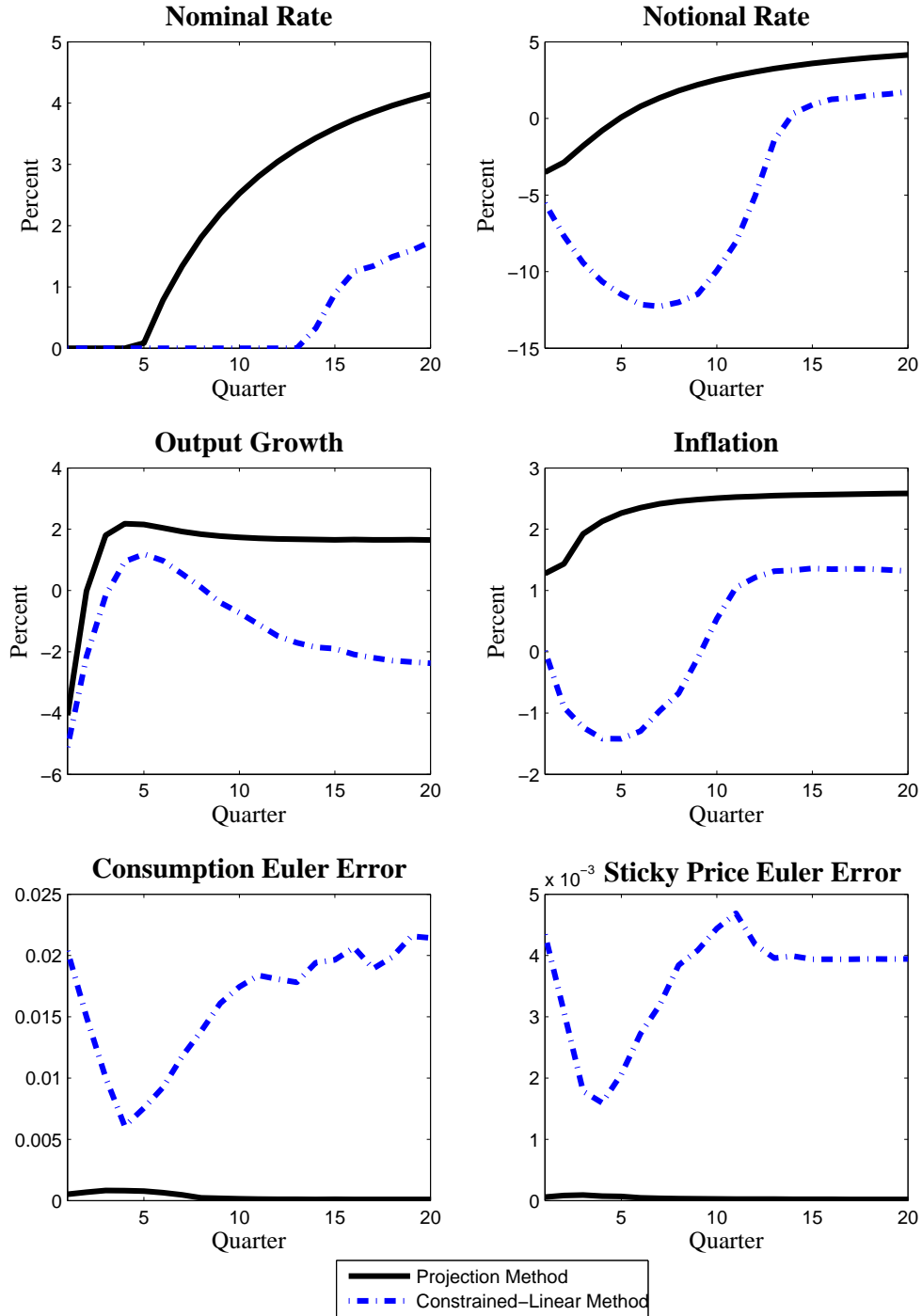
To compute our surrogate density we linearize the equations (12)-(14) and use a Kalman filter to compute the likelihood function, call it $p_{linear}(\mathbb{Y}_{1:T} | \vartheta)$, along with some surrogate prior over variables in ϑ , $p_{surrogate}(\vartheta)$, we construct our surrogate $\tilde{p}(\vartheta | \mathbb{Y}_{1:T}) \propto (p_{linear}(\mathbb{Y}_{1:T} | \vartheta) p_{surrogate}(\vartheta))^{\frac{1}{\mathcal{T}}}$, where \mathcal{T} is a tuning parameter (the temperature) that controls how much the surrogate model should guide the algorithm. We used $\mathcal{T} = 5$ for our surrogate, with insignificant differences between those estimates and ones produced with $\mathcal{T} = 6$ and $\mathcal{T} = 10,000$. The surrogate prior was either slightly more diffuse or the same as the prior used in the target density. We also noticed that the measurement errors produced by the surrogate differed substantially from that of the nonlinear model so that we added some auxiliary measurement error standard deviations ($\sigma_{\Delta y}^l, \sigma_{\pi}^l, \sigma_r^l$) to be used in linear likelihood computation.

B.3 The Surrogate Density

In this subsection, we report the results of 500,000 draws from our surrogate target density $\tilde{p}(\vartheta | \mathbb{Y}_{1:T})$ using a random walk Metropolis-Hastings algorithm, as well as the results from a density constructed using $p_{linear}(\vartheta | \mathbb{Y}_{1:T}) \propto p_{linear}(\vartheta | \mathbb{Y}_{1:T}) p(\vartheta)$ (not tempered). For the algorithm described in the main text to produce draws from the correct distribution, a support condition is needed, $supp\{p(\vartheta | \mathbb{Y}_{1:T})\} \subseteq supp\{\tilde{p}(\vartheta | \mathbb{Y}_{1:T})\}$. Inspecting marginal densities, it appears that the support of the surrogate density contains that of the target density.²⁹ The posterior density constructed by the linearized model differs from the target in economically meaningful ways, prices are less sticky, monetary policy reacts much less strongly to inflation, as well as the persistence of the η shock is much higher. Notwithstanding these differences, with an appropriate amount of tempering, we can exploit this approximation to the nonlinear model's likelihood function to substantially speedup the run-time of our algorithm.

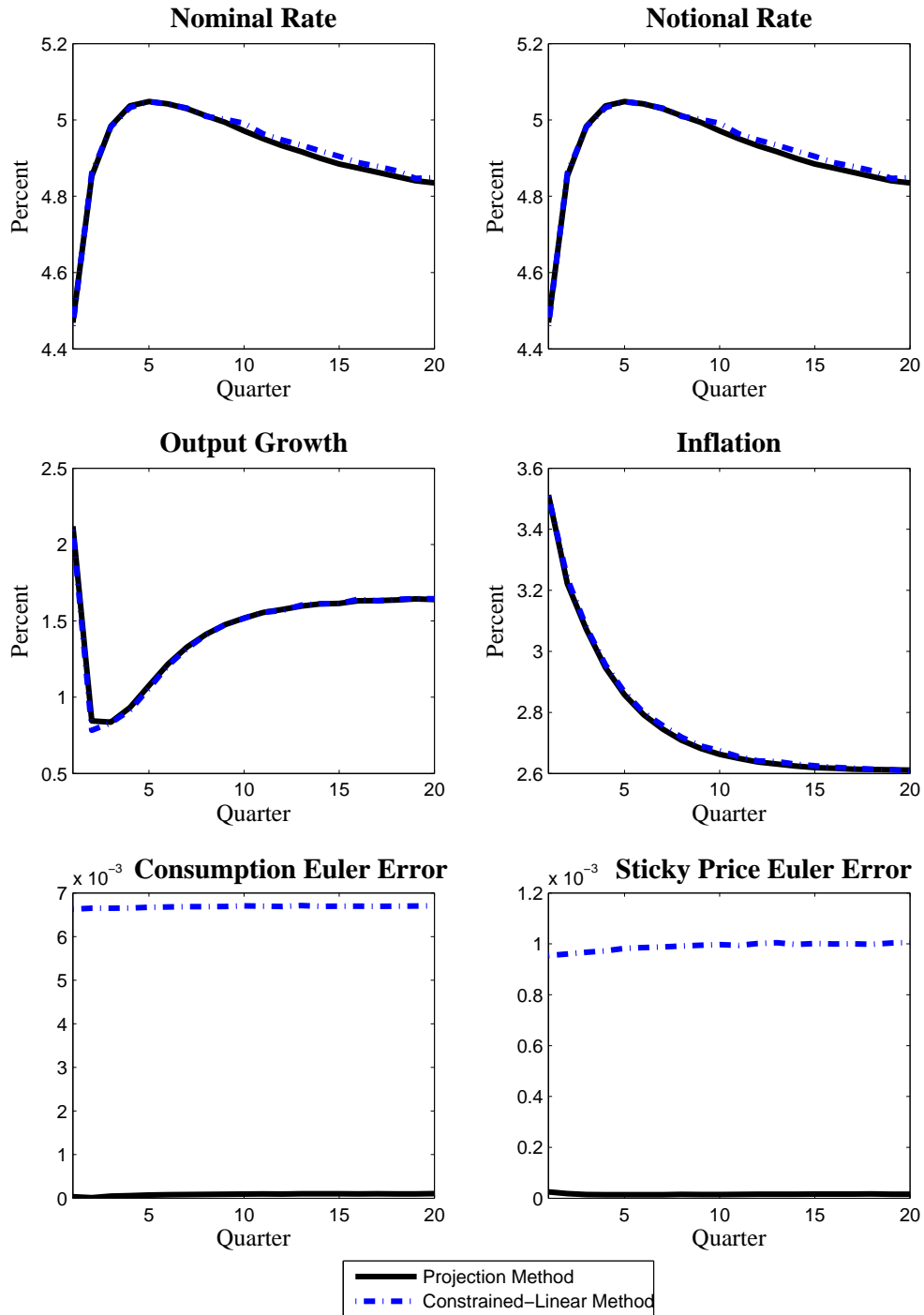
²⁹For this exercise, we fix the parameters G and π at the mean of the GDP growth and inflation series, respectively. The actual surrogate evaluates the linear model at those means, but draws new G and π from a dispersed Normal prior. As a check, 99% confidence bands were compared and found no issues with the support of surrogate not encompassing that of the target density.

Figure B.1: Comparison of Model Solutions (2009:Q2 Initial Conditions)



Note: For each solution method, the responses are computed using the posterior means of the parameter values, and the mean estimate of the state as initial conditions in 2009:Q2. We then simulate 1,000,000 paths and report the median value across these paths for each variable in each period.

Figure B.2: Comparison of Model Solutions (2006:Q1 Initial Conditions)



Note: For each solution method, the responses are computed using the posterior means of the parameter values, and the mean estimate of the state as initial conditions in 2006:Q1. We then simulate 1,000,000 paths and report the median value across these paths for each variable in each period.

Table B.1: Linearized Posterior

	mean	stdev	0.025	0.975
β	0.9987	0.0000	0.9987	0.9987
γ	0.5732	0.0683	0.4326	0.6994
φ	83.0883	14.7003	56.8887	114.2525
ε	6.0000	0.0000	6.0000	6.0000
γ_π	0.5156	0.0635	0.4030	0.6512
γ_Y	0.1707	0.0299	0.1165	0.2341
ρ_R	0.8834	0.0270	0.8297	0.9353
ρ_η	0.9145	0.0255	0.8629	0.9631
σ_Z	0.0176	0.0027	0.0131	0.0235
σ_R	0.0018	0.0002	0.0015	0.0021
σ_η	0.0024	0.0003	0.0019	0.0031
G	1.0043	0.0000	1.0043	1.0043
$\bar{\Pi}$	1.0061	0.0000	1.0061	1.0061
σ_y^{ME}	0.0005	0.0001	0.0004	0.0008
σ_π^{ME}	0.0006	0.0002	0.0004	0.0010
σ_r^{ME}	0.0004	0.0000	0.0003	0.0005

Table B.2: Surrogate (Temperature=5)

	mean	stdev	0.025	0.975
β	0.9987	0.0000	0.9987	0.9987
γ	0.5476	0.1836	0.1696	0.8928
φ	100.3052	36.4111	41.4149	182.1303
ε	6.0000	0.0000	6.0000	6.0000
γ_π	0.7963	0.3672	0.3736	1.8523
γ_Y	0.2091	0.1148	0.0442	0.4908
ρ_R	0.8542	0.0782	0.6761	0.9815
ρ_η	0.8930	0.0624	0.7529	0.9892
σ_Z	0.0182	0.0114	0.0073	0.0472
σ_R	0.0022	0.0006	0.0014	0.0037
σ_η	0.0029	0.0012	0.0016	0.0060
G	1.0043	0.0000	1.0043	1.0043
$\bar{\Pi}$	1.0061	0.0000	1.0061	1.0061
σ_y^{ME}	0.0012	0.0012	0.0003	0.0047
σ_π^{ME}	0.0011	0.0005	0.0003	0.0022
σ_r^{ME}	0.0005	0.0002	0.0003	0.0008